Expectations over fractal sets: CARMA/SigmaOpt Seminar

David H. Bailey, Jonathan M. Borwein, Richard E. Crandall, Michael G. Rose

August 13, 2012

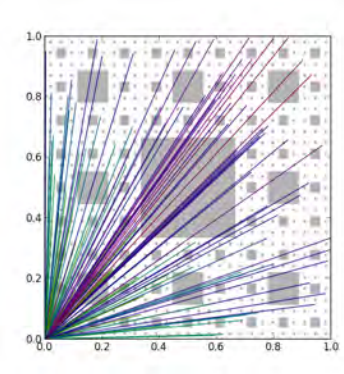

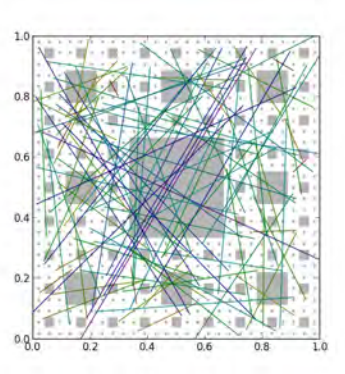

Abstract. Using fractal self-similarity and functional-expectation relations, the classical theory of box integrals—being expectations on unit hypercubes—is extended to encompass a new class of fractal "string-generated Cantor sets" (SCSs) embedded in unit hypercubes of arbitrary dimension. Motivated by laboratory studies on the distribution of brain synapses, these SCSs were designed for dimensional freedom—a suitable choice of generating string allows for fine-tuning the fractal dimension of the corresponding set. We also establish closed forms for certain statistical moments on SCSs, develop a precision algorithm for high embedding dimensions, and report various numerical results. The underlying numerical quadrature issues are in themselves quite challenging.

- The associated paper is at http://www.carma.newcastle.edu.au/jon/papers.html#PAPERS.

My main collaborators and some background

David Bailey

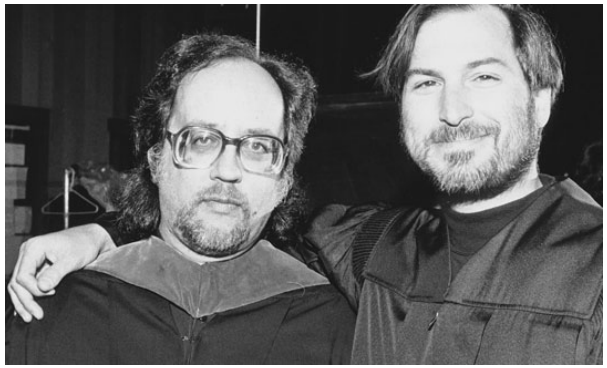

Richard Crandall and some Steve

Michael Rose

Before turning to these results, I briefly describe our prior work on Box integrals and some of the motivation for the current study.

1. *Exploratory experimentation* in mathematics: http://www.sciencedaily.com/releases/2011/10/111013085225.htm and http://www.ams.org/notices/201110/rtx111001410p.pdf (*Notices AMS* 2011)

2. High precision evaluation of physically meaningful integrals [6] and the hunt for *hyper-closed* forms: http://www.carma.newcastle.edu.au/jon/closed-form.pdf (*Notices AMS* 2012 in press)

3. Classical box integrals: *expectations* and moments are hyper-closed for dimension five or less (but only for cubes—all sides equal) [2,3,9]

4. Human wiring, rodent neurons and diagnosis of Alzheimer's disease [10, 11] and http://www.sciguru.com/newsitem/13858/how-mathematics-can-reveal-brain-structure-and-diagnose-brain-health

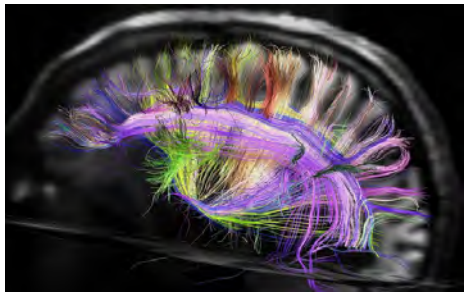

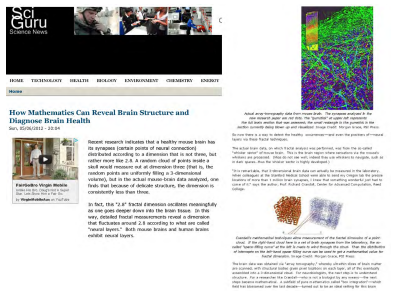

How Mathematics Can Reveal Brain Structure and Diagnose Brain Health

Sun, 05/06/2012 - 20:04

Recent research indicates that a healthy mouse brain has its synapses (certain points of neural connection) distributed according to a dimension that is not three, but rather more like 2.8. A random cloud of points inside a skull would measure out at dimension three (that is, the random points are uniformly filling a 3-dimensional volume), but in the actual mouse-brain data analyzed, one finds that because of delicate structure, the dimension is consistently less than three.

In fact, this "2.8" fractal dimension oscillates meaningfully as one goes deeper down into the brain tissue. In this way, detailed fractal measurements reveal a dimension that fluctuates around 2.8 according to what are called "neural layers." Both mouse brains and human brains exhibit neural layers.

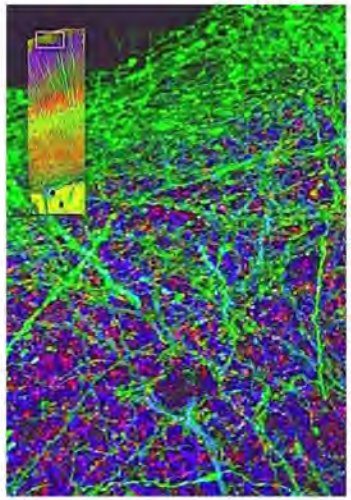

Actual array-tomography data from mouse brain. The synapses analyzed in the new research paper are red dots. The "gumstick" at upper left represents the full brain section that was assessed; the small rectangle in the gumstick is the section currently being blown up and visualized. Image Credit: Morgan Grace, PSI Press.

So now there is a way to detect the healthy occurrences---and even the positions of---neural layers via these fractal techniques.

The actual brain data, on which fractal analysis was performed, was from the so-called "whisker sector" of mouse brain. This is the brain region where sensations via the mouse's whiskers are processed. (Mice do not see well; indeed they use whiskers to navigate, such as in dark spaces...thus the whisker sector is highly developed.)

"It is remarkable, that 3-dimensional brain data can actually be measured in the laboratory. When colleagues at the Stanford Medical School were able to send my Oregon lab the precise locations of more than 1 million brain synapses, I knew that something wonderful just had to come of it." says the author, Prof. Richard Crandall, Center for Advanced Computation, Reed College.

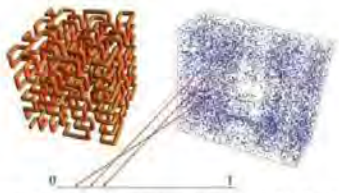

Crandall's mathematical techniques allow measurement of the fractal dimension of a point-cloud. If the right-hand cloud here is a set of brain synapses from the laboratory, the so-called "space-filling curve" at the left is made to wind through the cloud. Then the distribution of intercepts on the left-hand space-filling curve can be used to get a mathematical value for fractal dimension. Image Credit: Morgan Grace, PSI Press.

The brain data was obtained via "array tomography," whereby ultrathin slices of brain matter are scanned, with structural bodies given pixel locations on each layer, all of this eventually assembled into a 3-dimensional cloud. For neurobiologists, the next step is to understand structure. For a researcher like Crandall---who is not a biologist by any means---the next steps became mathematical. A subfield of pure mathematics called "box integration"---which field has blossomed over the last decade---turned out to be an ideal setting for this brain

1 Introduction

The development of the following mathematics was motivated by recent laboratory data concerning the spatial locations of 10^6 mouse-brain synapses naturally embedded in three dimensions. The synapses were found to be distributed in a fractal manner, with fractal box dimension strictly less than the limiting value of 3 that would be expected from a set of points randomly distributed throughout a cuboid (see [10] for full details and [14] for a recent popular account).[1]

Another way that laboratory distributions loom non-random is that statistical moments, such as expected pairwise distances, do not follow the statistics of random distributions. Indeed, the aforementioned brain data possesses certain expectations from non-random distributions. To understand such phenomena further, we develop herein various statistical measures—in particular, separation moments (box integrals)—on a particular class of abstract fractal sets, in the hope that these measures can assist the identification of empirical synapse distributions.

Box integrals were first introduced in 1976 as a means of analysing the expected norm on points uniformly distributed through unit hypercubes [1]. Following intensive study over the last decade, a number of closed-form results pertaining to box integrals have been developed; see for example [2], [3] and [9]. The canonical definitions are as follows [3].

Definition 1. *Given dimension n, complex parameter s and a fixed point q in the unit n-cube, the* box integral *$X_n(s,q)$ is defined as the expectation of a certain norm $|r-q|^s$, with q fixed and r chosen at random from a uniform distribution over the unit n-cube. That is,*

$$X_n(s,q) := \langle |r-q|^s \rangle_{r\in[0,1]^n} = \int_{r\in[0,1]^n} |r-q|^s \; \mathcal{D}r \tag{1}$$

where $\mathcal{D}r := dr_1 \ldots dr_n$ is the n-space volume element.

[1] The brain-synapse work to which we refer uses cuboids, being right-parallelepipeds of sides (a,b,c), for which box integrals are taken over the volume abc. In the present treatment, we restrict our study to the n-cube $[0,1]^n$ and fractal sets embedded in such cubes.

Example 1. Three classically important instances of the X-integrals are:

1. $B_n(s)$, the order-s moment of separation between a random point and a vertex of the n-cube (such as the origin):

$$B_n(s) \;:=\; X_n(s,0) \;=\; \int_{r\in[0,1]^n} |r|^s \; \mathcal{D}r; \tag{2}$$

2. $\Gamma_n(s)$, the order-s moment of separation between a random point and the centroid $\mathbf{1/2} = (1/2, 1/2, \ldots, 1/2)$ of the n-cube:

$$\Gamma_n(s) \;:=\; X_n(s,\mathbf{1/2}) \;=\; \int_{r\in[0,1]^n} |r-\mathbf{1/2}|^s \; \mathcal{D}r; \tag{3}$$

3. $\Delta_n(s)$, the order-s moment of separation between *two* random points in the n-cube:

$$\Delta_n(s) \;:=\; \langle X_n(s,q)\rangle_{q\in[0,1]^n} \;=\; \int_{r,q\in[0,1]^n} |r-q|^s \; \mathcal{D}r\mathcal{D}q. \tag{4}$$

It is these three expectations which we aim to generalize, with particular emphasis placed on $\Delta_n(s)$ as the measure most relevant to the analysis of empirical synapse distributions. ◇

The existence of well-defined analytic continuations for $B_n(s)$ and $\Delta_n(s)$ over the complex s-plane was established in [2] and [3]. In particular, $B_n(s)$ was found to have the following absolutely convergent analytic series:

$$B_n(s) \;=\; \frac{n^{1+s/2}}{s+n}\sum_{k=0}^{\infty}\gamma_{n-1,k}\left(\frac{2}{n}\right)^k \tag{5}$$

where the $\gamma_{m,k}$ are fixed coefficients defined by the following two-variable recursion [11]:

$$(1+2k/m)\gamma_{m,k} \;=\; (k-1-s/2)\gamma_{m,k-1}+\gamma_{m-1,k} \tag{6}$$

for $m,k\geq 1$; this recursion being ignited by $\gamma_{0,k}:=\delta_{0,k}$, $\gamma_{m,0}:=1$. Of particular interest to the present work is the fact that the analytic series (5) exhibits a pole at $s=-n$, the negated dimension of the sample space (cf Theorem 5).

The goal of this paper is to establish a solid theoretical foundation and closed form results for box integrals over a restricted class of fractal sets; namely, what we call string-generated Cantor sets (SCSs). These sets are formally introduced in Section 2 and a closed form is provided for the relationship between their fractal dimensions and generating strings. We begin to extend the classical box integrals $B_n(s)$, $\Gamma_n(s)$ and $\Delta_n(s)$ over the SCSs in Section 3, using a heuristic notion of expectation.

A spectral formalism is brought to bear in Section 4. This with the addition of fractal self-similarity relations developed in Section 5 enables closed forms for the expectations to be obtained. Exact results are obtained for arbitrary moments in embedding-dimension one in Section 6, and for second moments in arbitrary dimensions in Section 7. Self-similarity relations are used to analyse the complex poles of $B_n(s)$ (as defined over SCSs) in Section 8. We finish with some numerical results and open questions in Section 9. Some numerical data and plots regarding the fractal dimensions and second-order separation moments on various SCSs in Appendix A—along with a discussion of the methods employed.

Let us emphasise that in this paper we take very much a physicist's view of the expectations we will uncover. We leave the considerable work of producing a mathematically rigorous accounting (in terms of abstract measure theory) for a subsequent paper.

2 String-generated Cantor sets

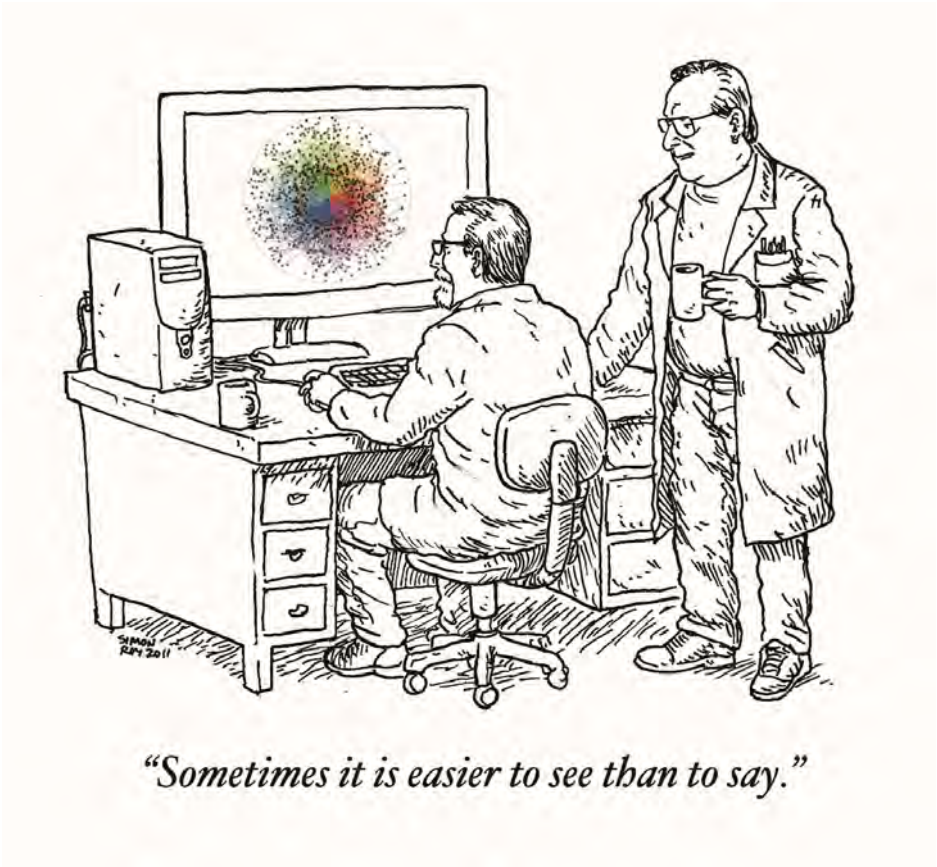

‘

As a first step towards the full generalisation of classical box integrals to arbitrary fractal sets, we introduce the concept of a *string-generated Cantor set* (SCS). Though our definition will perhaps appear arbitrary, or not general enough, our motive was simply to construct a class of Cantor-like fractals embedded in dimension n with controllable *fractal box dimension* [4] lying in some convenient interval. The brain-synapse research in [10] showed that experimental fractal dimensions tended to be near $n = 3$ for the 3-dimensional data, yet *varying* along the penetration axis of the tissue. Thus a fractal model is motivated in which one may "tune" the dimension as required. ◇

2.1 Formal Definition of a String-generated Cantor Set

The complete structure of any SCS is encoded within its generating string. For known embedding dimension n, let $P = P_1P_2 \dots P_p$ denote a periodic string of digits with period p, some positive integer. For instance, with $n = 1$, $P = 01$ will denote the period-2 string $\overline{01} = 010101\dots$ (the over-line being henceforth omitted from our notation for convenience). In the embedding space $[0,1]^n$ we will consider only those strings for which $P_i \leq n$ for all i. This restriction enables us to define a family of SCSs embedded in the unit n-cube for a given embedding dimension n.

Consider the ternary expansion for coordinates of $x = (x_1, \dots, x_n) \in [0,1]^n$, namely:

$$\begin{aligned} x_1 &= 0\,.\,x_{11}\ x_{12}\ x_{13}\dots \\ x_2 &= 0\,.\,x_{21}\ x_{22}\ x_{23}\dots \\ &\vdots \\ x_n &= 0\,.\,x_{n1}\ x_{n2}\ x_{n3}\dots \\ &\quad\ \uparrow\ \ \uparrow\ \ \uparrow \\ &\quad\ c_1\ \ c_2\ \ c_3\ \ \dots \end{aligned}$$

with every digit $x_{jk} \in \{0,1,2\}$ (or, when working with "balanced" ternary vectors, $x_{jk} \in \{-1,0,1\}$) and the vectors $c_k = (x_{1k}, \dots, x_{nk})$ denoting respective columns of digits. Each periodic string defines an SCS by singling out points with admissible ternary expansions (the SCS being the collection of such admissible points). More precisely, in a given generating string P the value of P_k determines the maximum number of coordinates of x that are permitted to have the digit 1 in the kth (and $(k+p)$th, $(k+2p)$th, ...) place of the ternary expansion.

For the purpose of enumerating the digits that are restrained by the generating strings, we define the following counting functions. First, the "unit" counter, appropriate to vectors c having all elements $\in \{0, 1, 2\}$:

$$U(c) \;:=\; \#\{1\text{'s in ternary vector } c\},$$

and for later use with balanced ternary vectors b having all elements $\in \{-1, 0, 1\}$, the "zero" counter:

$$Z(b) \;:=\; \#\{0\text{'s in ternary vector } b\}.$$

(Typically we create a balanced-ternary vector b from a standard ternary vector c simply by $b = c - (1, 1, 1, \dots)$.)

We are now ready to formally define a string-generated Cantor set.

Definition 2. *Fix positive integers n and p. Given an embedding space $[0, 1]^n$ and an entirely-periodic string $P = P_1 P_2 \dots P_p$ of non-negative integers with $P_i \leq n$ for all $i = 1, 2, \dots, p$, the* String-Generated Cantor Set (SCS)*, denoted $C_n(P)$, is the set of all admissible $x \in [0, 1]^n$, where*

$$x \text{ admissible} \iff U(c_k) \leq P_k \quad \forall\, k \in \mathbb{N} \tag{7}$$

with notational periodicity assumed: $P_{p+k} := P_k$ for all $k \geq 1$.

Remark 1. We make the following preliminary observations:

1. $C_1(0)$ is the classical "middle-thirds-removed" Cantor set on $[0,1]$, as a point $x \in C_1(0)$ is defined to be admissible iff its ternary expansion is entirely devoid of 1's (i.e. $U(c_k) \leq 0$).

2. $C_n(n)$ is the full unit n-cube $[0,1]^n$, as all points $x \in [0,1]^n$ are admissible (every ternary vector is allowed for every column c_k).

3. For a fixed embedding dimension n, if a single element $P_k < n$ of a periodic string P is increased, the restrictions on admissible points are relaxed and so the resulting SCS contains the original SCS. Every SCS $C_n(P)$ contains the maximally-restricted SCS, $C_n(0)$, and is contained by the full n-cube, $C_n(n)$ (which places no restrictions on admissible points).

4. The Lebesgue measure of (the always uncountable set) $C_n(P)$ is zero *unless* $P = n$, in which case the Lebesgue measure is n (since the SCS is exactly the full n-cube)—this follows from the Borel Zero-One law [5].[2]

Some pictorial examples of various string-generated Cantor sets in one, two and three dimensions are shown in Figure (2.1). ◇

[2] A brief outline of the argument, which generalises to higher dimensions n, is as follows. A point chosen at random from the set $C_1(0)$ is admissible only if the digit 1 is avoided in every position of the ternary expansion. The probability that this occurs at each appropriate digit in the expansion is 2/3, and

$$\sum_{n=1}^{\infty} \left(\frac{2}{3}\right)^n = 2 < \infty$$

so the Borel Zero-One law implies a zero probability of admissibility—and a Lebesgue measure 0 by definition (over strings). Uncountability follows immediately upon mapping digits $0 \to 0$, $2 \to 1$, so the cardinality of $C_1(0)$ is that of $[0,1]$.

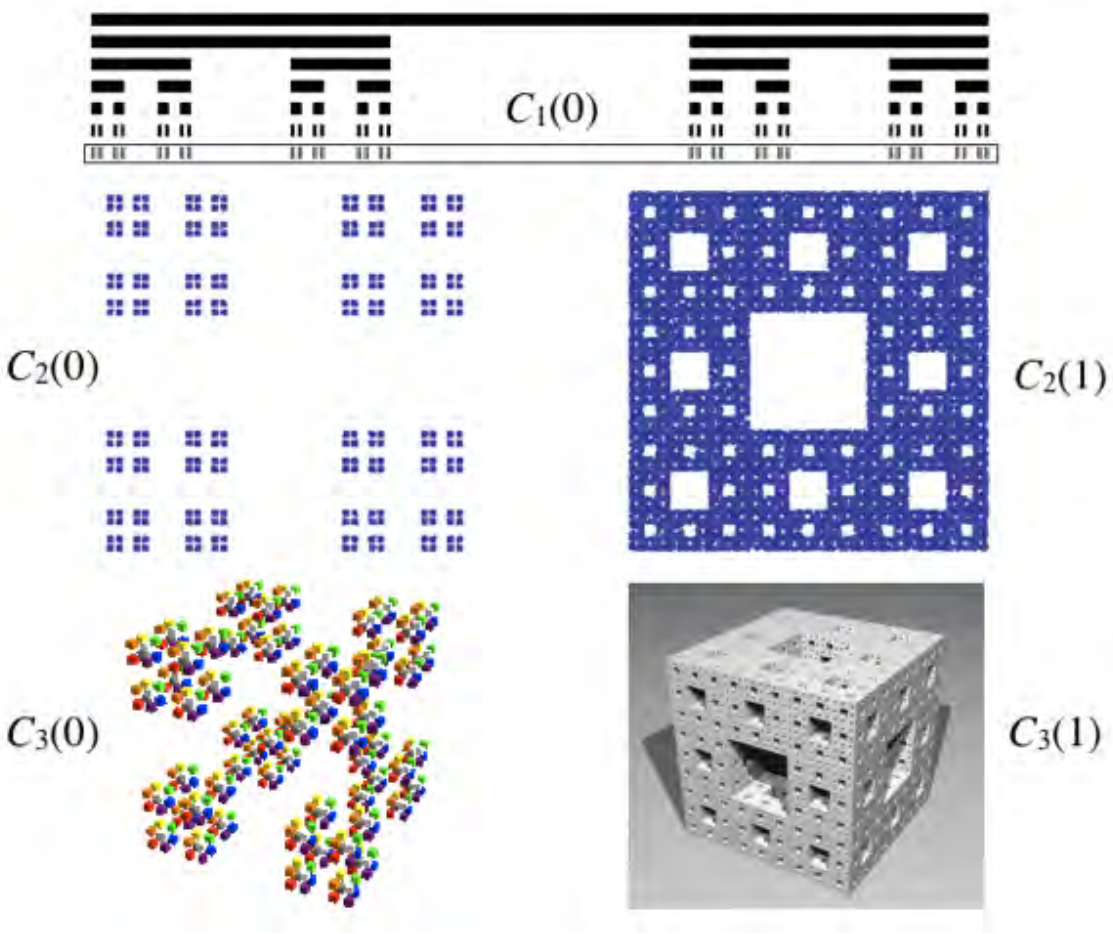

Figure 1: Various renderings of string-generated Cantor sets (SCSs), showing dependence on the defining string and different styles of visualization. The upper image shows the 'middle-thirds-removal' procedure for generating the standard Cantor set $C_1(0)$ of dimension $\log_3 2$—the thin, wide rectangle showing the 'dusty' set remaining after 6 recursive removals. At middle left is $C_2(0)$—sometimes called 'Cantor dust', of dimension $\log_3 4$. Middle right shows another 2-dimensional variant, $C_2(1)$—sometimes called a 'gasket', of dimension $\log_3 8$. Lower-left shows $C_3(0)$, also of dimension $\log_3 8$ (image due to A. Baserinia (2006)) and lower-right shows $C_3(1)$, of dimension $\log_3 20$ (image due to R. Dickau (2008)).

2.2 Fractal dimension of an SCS

The periodic string formulation in Definition 2 immediately gives rise to a closed form for the fractal dimension of an SCS.[3]. The proof of this closed form result utilises the machinery of iterated function systems, which we briefly introduce below [13].

Definition 3. *A mapping* $S : \mathbb{R}^n \to \mathbb{R}^n$ *is a* contraction *if there exists a* contraction factor $0 < c < 1$ *such that* $|S(x) - S(y)| \leq c|x - y|$ *for all* $x, y \in \mathbb{R}^n$. *If equality holds for all* x *and* y, *the mapping is said to be a* similarity. *An* iterated function system (IFS) *is a finite family of contractions* $\{S_1, S_2, \ldots, S_m\}$ *with* $m \geq 2$. *Every IFS has a unique* attractor - *a non-empty compact subset* $A \subset \mathbb{R}^n$ *such that*

$$A = \bigcup_{i=1}^{m} S_i(A)$$

An IFS is said to satisfy the open set condition *if there exists a non-empty bounded open set* $V \subset \mathbb{R}^n$ *such that*

$$V \supset \bigcup_{i=1}^{m} S_i(V)$$

Theorem 1 (Fractal dimension of a self-similar set). *Suppose that the open set condition holds for the IFS* $\{S_1, S_2, \ldots, S_m\}$ *on* $\mathbb{R}^n$ *(with associated contraction factors* $\{c_1, c_2, \ldots, c_m\}$*). Then the Hausdorff dimension and box-counting dimension of the IFS attractor are equal and take the value* δ, *where:*

$$\sum_{i=1}^{m} (c_i)^{\delta} = 1 \tag{8}$$

[3] In this paper, the phrase "fractal dimension" will always refer to both the Hausdorff and box-counting dimensions [13, Chapters 2 & 3], which are shown to be identical for any given SCS in the proof of Proposition 7

As a final preliminary observation, note that for a given periodic string P the set of admissible columns c_k is enumerated by the formula:

$$N_k(P,n) := N_k = \#\{\text{admissible columns } c_k\} \;=\; \sum_{j=0}^{P_k} \binom{n}{j} 2^{n-j}, \tag{9}$$

which follows directly from the observation that $j \leq P_k$ coordinates may attain the value 1, leaving $n-j$ positions each able to attain the value 0 or 2. Note also that the minimum fractal dimension (corresponding to the sparsest SCS) has $N_k = 2^n$, while the maximum dimension (corresponding to the unit n-cube) has $N_k = 3^n$.

Proposition 1 (Fractal dimension—closed form). *The fractal dimension (in both the Hausdorff and box-counting sense) $\delta(C_n(P))$ of the SCS $C_n(P)$ is given by the closed form*

$$\delta\left(C_n(P)\right) \;=\; \frac{\log \prod_{k=1}^{p} N_k(P,n)}{p \log 3}. \tag{10}$$

Proof. The set $C_n(P)$ can be thought of as the union of finitely many copies of itself scaled by a factor of 3^{-p} (cf figure 2.1). Overlay the unit n-cube with 3^p hypercubes of side length 3^{-p} and consider the similarities S_i that map the unit n-cube into these hypercube subsets. Note that all such similarities have contraction factor 3^{-p}. The IFS with attractor $C_n(P)$ consists of those 'admissible' similarities S_i which map the unit n-cube into a hypercube subset that intersects $C_n(P)$. To enumerate these admissible similarities we use our column-counting formula (9).

Consider the fractal approximation set to $C_n(P)$ obtained by truncation of the periodic string P to its first p digits (ie. its first complete period). This approximation set is identical to $C_n(P)$ on scales greater than 3^{-p}, but contains no fine structure below this limit. Equivalently, consider the equivalence classes containing those points in the unit n-cube whose coordinate ternary expansions are all equal up to and including the p-th digit. Each equivalence class (which can be represented by a coordinate ternary expansion consisting of all 0's after the p-th place) can be mapped one-to-one onto its own 3^{-p}-scaled hypercube. The number of such hypercubes that intersect $C_n(P)$—and thus the number of admissible similarities—is therefore equal to the number of admissible equivalence classes. Each admissible equivalence class corresponds to a ordered concatenation of admissible c_k columns for $k = 1, \ldots, p$.

For the kth ternary place there are N_k admissible columns c_k, so the number of admissible similarities is enumerated by:

$$m = \prod_{k=1}^{p} N_k.$$

Assign each admissible similarity an unique index i ranging from 1 to $m = \prod N_k$ (the product ranging from $k = 1$ to p). Then, the self-similar structure of $C_n(P)$ is encapsulated by

$$C_n(P) = \bigcup_{i=1}^{\prod N_k} S_i(C_n(P))$$

The similarities S_i satisfy the open set condition if V is taken as the interior of the unit n-cube.

It remains to verify the summation in (8) for our claimed closed form for δ:

$$\begin{aligned}\sum_{i=1}^{m}(c_i)^{\delta} &= \sum_{i=1}^{\prod N_k}\left(3^{-p}\right)^{\frac{\log\prod N_k}{p\log 3}}\\ &= \prod N_k\left(3^{-\log_3\prod N_k}\right)\\ &= 1\end{aligned}$$

Having satisfied all the conditions of Theorem 1, the result immediately follows. □

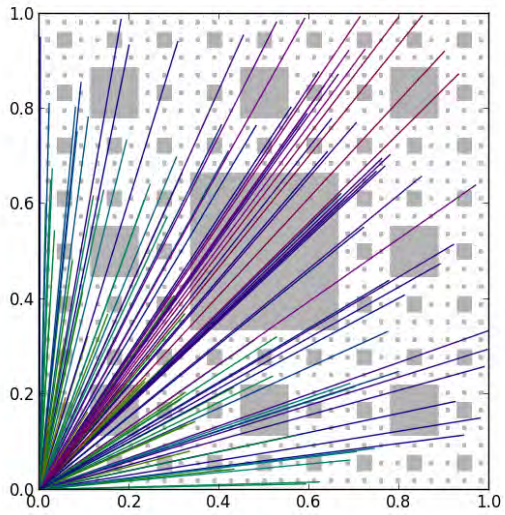

$$B(2, C_2(1)) = \frac{11}{16} = 0.6875$$

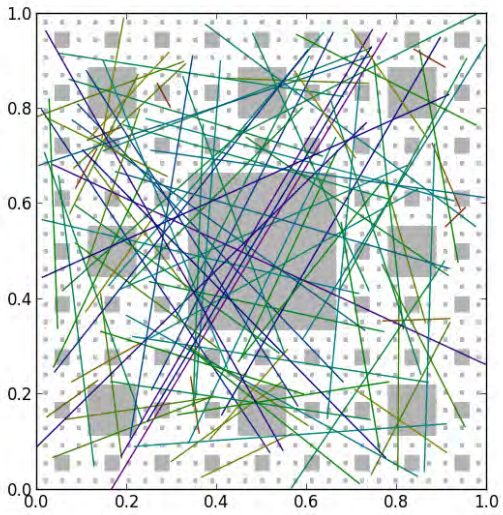

$$\Delta(2, C_2(1)) = \frac{3}{8} = 0.375$$

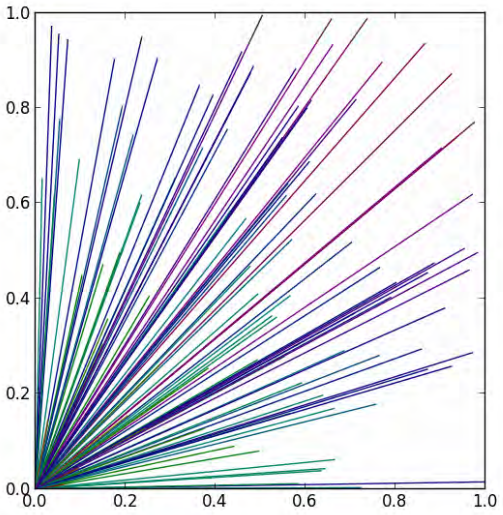

$$B(2, C_2(2)) = \frac{2}{3} = 0.66\ldots$$

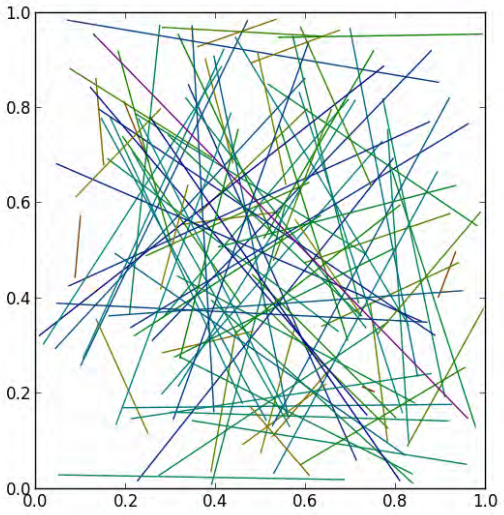

$$\Delta(2, C_2(2)) = \frac{1}{3} = 0.33\ldots$$

Figure 2: Sampling distances in the Sierpinski carpet $C_2(1)$ and unit square $C_2(2)$ (left), and expectation of a 3-step random walk (right)

Example 2. Note that the fractal dimension $\delta(C_n(P))$ of the SCS $C_n(P)$dimension $\delta(C_n(P))$ depends only on the embedding dimension n and the generating string $P = (P_1 \dots P_p)$, as exemplified by the following:

1. The dimension of the full unit n-cube comes out to be $\delta(C_n(n)) = n$, as expected.

2. The dimension of the classical Cantor set comes out to be the celebrated result

$$\delta(C_1(0)) \;=\; \log_3(2).$$

3. In $n = 6$ embedding dimensions, the Cantor set $C_6(1012)$ has dimension

$$\delta(C_6(1012)) \;=\; \frac{26\log 2 + \log 31}{4\log 3} \;\approx\; 4.8848.$$

4. We can derive arbitrary-dimension formulae for a given string P. For example, when $P = 2$ (and $n \geq 2$):

$$\delta(C_n(2)) \;=\; \log_3(2^{n-3}(n^2 + 3n + 8)).$$

Remark 2. Note also that the fractal dimension $\delta(C_n(P))$ of the SCS $C_n(P)$ depends only on the elements present in the generating string, and *not* the order in which they occur. This has a nice consequence for modelling applications—permuting the generating string of an SCS allows for fine-tuning of the statistical measures without altering the fractal dimension of the model. ◇

2.3 Density theorem for SCS fractal dimensions

The range of available fractal dimensions in any given class of SCSs is quantified by the following proposition, which is a straightforward deduction from the explicit formula (10). Recall that the minimum fractal dimension for a given embedding space has $N_k = 2^n$, while the maximum dimension has $N_k = 3^n$.

Proposition 2. *For given embedding dimension n, the set of possible fractal dimensions $\delta(C_n(P))$ is dense on the interval $[n \log_3 2, n]$.*

Proposition 2 ensures that for 3-dimensional embedding we can always select some SCS in order to exhibit a fractal dimension numerically anywhere in the interval $[1.90, 3.00]$. The motivating research in [10] experimentally requires this sort of span—certainly the interval $[2.4, 3.0]$—as brain-synapse dimensions vary importantly across neural layers. Indeed the simple form $\delta\left(C_n(P)\right) = (\log_3 \prod_{k=1}^{p} N_k)/p$ has various computational applications, such as "matching" an SCS to an actual laboratory distribution.

n	s	$B(s, C_2(2))$
2	-4	$-\frac{1}{4} - \frac{\pi}{8}$
2	-3	$-\sqrt{2}$
2	-2	∞
2	-1	$2\log(1+\sqrt{2})$
2	1	$\frac{1}{3}\sqrt{2} + \frac{1}{3}\log(1+\sqrt{2})$
2	3	$\frac{7}{20}\sqrt{2} + \frac{3}{20}\log(1+\sqrt{2})$
n	s	$B(s, C_3(3))$
3	-5	$-\frac{1}{6}\sqrt{3} - \frac{1}{12}\pi$
3	-4	$-\frac{3}{2}\sqrt{2}\arctan\frac{1}{\sqrt{2}}$
3	-3	∞
3	-2	$-3G + \frac{3}{2}\pi\log(1+\sqrt{2}) + 3\ \mathrm{Ti}_2(3-2\sqrt{2})$
3	-1	$-\frac{1}{4}\pi + \frac{3}{2}\log\left(2+\sqrt{3}\right)$
3	1	$\frac{1}{4}\sqrt{3} - \frac{1}{24}\pi + \frac{1}{2}\log\left(2+\sqrt{3}\right)$
3	3	$\frac{2}{5}\sqrt{3} - \frac{1}{60}\pi + \frac{7}{20}\log\left(2+\sqrt{3}\right)$

Table 1: Evaluations for $B_{2,3}(s)$. For $C_n(n)$ all integer values for $1 \le n \le 5$ have closed forms. Ti_2 is a generalized tangent (polylog) value and G is Catalan's constant.

2.4 Expectations for the full cube

In Tables 1 and 2 we show various results for expectations over the *full* cube in two and three dimensions as established in [2]. The evaluations are hypergeometric in stark contrast with our later rationality results such as Corollary 2 of Section 8.4.

n	s	$\Delta(s, C_2(2))$
2	-5	$\frac{4}{3}+\frac{8}{9}\sqrt{2}$
2	-2,-3,-4	∞
2	-1	$\frac{4}{3}-\frac{4}{3}\sqrt{2}+4\log(1+\sqrt{2})$
2	1	$\frac{2}{15}+\frac{1}{15}\sqrt{2}+\frac{1}{3}\log(1+\sqrt{2})$
n	s	$\Delta(s, C_3(3))$
3	-7	$\frac{4}{5}-\frac{16\sqrt{2}}{15}+\frac{2\sqrt{3}}{5}+\frac{\pi}{15}$
3	–3,-4,-5,-6	∞
3	–2	$2\pi-12\ G+12\,\mathrm{Ti}_2\left(3-2\sqrt{2}\right)+6\pi\log\left(1+\sqrt{2}\right)$ $+2\log 2-\frac{5}{2}\log 3-8\sqrt{2}\arctan\left(\frac{1}{\sqrt{2}}\right)$
3	-1	$\frac{2}{5}-\frac{2}{3}\pi+\frac{2}{5}\sqrt{2}-\frac{4}{5}\sqrt{3}+2\log\left(1+\sqrt{2}\right)$ $+12\log\left(\frac{1+\sqrt{3}}{\sqrt{2}}\right)-4\log\left(2+\sqrt{3}\right)$
3	1	$-\frac{118}{21}-\frac{2}{3}\,\pi+\frac{34}{21}\,\sqrt{2}-\frac{4}{7}\,\sqrt{3}$ $+2\,\log\left(1+\sqrt{2}\right)+8\,\log\left(\frac{1+\sqrt{3}}{\sqrt{2}}\right)$
3	3	$-\frac{1}{105}-\frac{2}{105}\,\pi+\frac{73}{840}\,\sqrt{2}+\frac{1}{35}\,\sqrt{3}$ $+\,\frac{3}{56}\,\log\left(1+\sqrt{2}\right)+\frac{13}{35}\,\log\left(\frac{1+\sqrt{3}}{\sqrt{2}}\right)$

Table 2: Evaluations for $\Delta_{2,3}(s)$. For $C_n(n)$ all integer values for $1 \leq n \leq 5$ have closed forms.

3 Statistical definitions

In order to extend the classical box integrals of Section 1 to the string-generated Cantor sets defined in Section 2, we proceed from their interpretation as expectations over the unit n-cube. We will later connect the generalised box integrals $B(s, C_n(P))$, $\Gamma(s, C_n(P))$ and $\Delta(s, C_n(P))$ to explicit integrals over the unit n-cube; for now, we denote certain expectations over an arbitrary SCS $C_n(P)$ by the following formal assignments (after all, we have not yet defined *expectations* over an SCS): for $\Re(s) > 0$

$$B(s, C_n(P)) := \langle |r|^s \rangle_{r \in C_n(P)}, \tag{11}$$

$$\Gamma(s, C_n(P)) := \langle |r - \mathbf{1/2}|^s \rangle_{r \in C_n(P)}, \tag{12}$$

$$\Delta(s, C_n(P) := \langle |r - q|^s \rangle_{r,q \in C_n(P)}. \tag{13}$$

For now all we intend is the appropriate linearity of an expectation.

Remark 3. Note that we have suppressed the subscript n on B, Γ and Δ, since the embedding dimension n is now implicit in the choice of $C_n(P)$. Although expectations on a fractal SCS have yet to be defined, we will require from our definition that

$$B(s, C_n(n)) = B_n(s), \quad \Gamma(s, C_n(n)) = \Gamma_n(s) \quad \text{and} \quad \Delta(s, C_n(n)) = \Delta_n(s)$$

since $C_n(n)$ is always the full n-cube $[0, 1]^n$. ◇

3.1 Precise definition of expectation

For a complex-valued function $F : \mathcal{R}^n \to \mathcal{C}$ we consider the evaluations of F at every admissible point in an SCS and adopt the definition:

Definition 4. *The expectation of $F : \mathcal{R}^n \to \mathcal{C}$ on an SCS $C_n(P)$ is defined by*

$$\langle F(r) \rangle_{r\in C_n(P)} := \lim_{j\to\infty} \frac{1}{N_1 \cdots N_j} \sum_{U(c_i)\le P_i} F(c_1/3 + c_2/3^2 + \cdots + c_j/3^j),$$

$$\langle F(r-q) \rangle_{r,q\in C_n(P)} := \lim_{j\to\infty} \frac{1}{N_1^2 \cdots N_j^2} \sum_{U(c_i),U(d_i)\le P_i} F((c_1-d_1)/3 + \cdots + (c_j-d_j)/3^j),$$

when the respective limits exist.

It is possible to show that for moment functions such as $F(r) := |r|^s$ the defining limits exist, uniformly on compact sets with $\Re(s) \ge 0$ and so are analytic. We also allow ourselves analytic continuation beyond this half s-plane.[4]

In the next section we concern ourselves with establishing a probability measure such that, at least formally,

$$\langle F(r) \rangle_{r\in C_n(P)} = \int_{r\in[0,1]^n} F(r)\,\phi(r)\,\mathcal{D}r, \tag{14}$$

where ϕ is a probability density that vanishes on inadmissible $r \in [0,1]^n \setminus C_n(P)$. We have not started with such a measure-based definition for the simple reason that the ϕ tend to be pathological, as in mathematical physics when infinite "delta-function combs" emerge.[5]

[4] It is possible to alter this definition of expectation to allow some negative powers s. One way is to use "primed sums," whereby one never allows F arguments of the 0 vector on the right. Another way—for the first part of the definition—is to replace $c_1/3 + c_2/3^2 + \cdots + c_j/3^j \to c_1/3 + c_2/3^2 + \cdots + (c_j + \mathbf{1}/\mathbf{2})/3^j$, thereby offsetting slightly the argument vector to coincide with the centroid of a given admissibility box.

[5] Even for the 1-dimensional classical Cantor set $C_1(0)$, such a ϕ—a Cantor function derivative– must take infinite values on a fractal of measure 0 in order to satisfy the normalization requirement $\int \phi\, dr = 1$.

4 Spectral formalism of the SCS random walk

4.1 Random-walk approach

Let us view of the vector r (tested for admissibility along the lines of Definition (2)) as a random walk whose N-th step has position

$$r^{(N)} = c_1/3 + c_2/3^2 + \cdots c_N/3^N,$$

with $U(c_k) \leq P_k$.[6]. Then the *transition probability density* for displacement $u := r^{(k)} - r^{(k-1)}$ can be formally cast as

$$\tau_k(u) = \frac{1}{N_k} \sum_{U(c_k) \leq P_k} \delta^n(u - c_k/3^k).$$

The physical analogy here is simple: the random walk jumps to its k-th position according to a comb of n-dimensional delta functions (and note that $\int \tau(u)\, \mathcal{D}u = 1$). This random-walk picture is conceptually compatible with the expectation definition of Equation 4.

Now the transition density τ_k enjoys a Fourier transform

$$T_k(\omega) = \int \tau_k(u) e^{i\omega \cdot u}\, \mathcal{D}u,$$

where the integral is taken over R^n.

[6] Connections to formal lattice theory for random walks can be made if we restrict ourselves to only finitely many steps

4.2 The underlying density

The convolution principle then establishes—at least formally—that the random walk's overall density is

$$\phi(r) \;=\; \frac{1}{(2\pi)^n}\int \prod_{k=1}^{\infty} T_k(\omega)\, e^{-i\omega\cdot r}\, \mathcal{D}\omega. \tag{15}$$

This formal result turns out to be quite powerful if we carefully denote a *spectral kernel*

$$ {}_nG_P(\omega) \;:=\; \prod_{k=1}^{\infty} \frac{1}{N_k} \sum_{Z(b_k)\le P_k} e^{i\omega\cdot b_k/3^k}, \tag{16}$$

where it will be noted that we have transformed to *balanced ternary* vectors b_k—being vectors of elements $x_{jk} \in \{-1, 0, 1\}$, each vector having zero-count $Z(b_k)$ not exceeding P_k (see Definition 2). Note that $Z(b_k) = Z(|b_k|)$ where $|b_k|$ represents the coordinatewise absolute value. It is useful to observe that

$$ {}_nG_P(\omega) \;:=\; \prod_{k=1}^{\infty} \frac{1}{N_k} \sum_{Z(b_k)\le P_k} \cos(\omega\cdot b_k/3^k), \tag{17}$$

since $-b_k$ is admissible exactly when b_k is.

When it is clear from context we will denote $G_P := {}_nG_P$. With this notation in mind we have the fundamental density relation

$$\phi(r) \;=\; \frac{1}{(2\pi)^n}\int e^{-i\omega\cdot r} e^{i\omega\cdot \mathbf{1/2}} G_P(\omega)\, \mathcal{D}\omega, \tag{18}$$

and a similarly derived representation for the density Φ of a two-vector difference $r - q$:

$$\Phi(d := r - q) \;=\; \frac{1}{(2\pi)^n}\int e^{-i\omega\cdot d} |G_P(\omega)|^2\, \mathcal{D}\omega, \tag{19}$$

It is instructive (and as we shall see, lucrative) to observe that our spectral kernel has a simple interpretation as an expectation; that is, application of Definition 4 to (16) immediately yields

$$G_P(\omega) \;=\; \left\langle e^{i\omega\cdot(r-\mathbf{1/2})}\right\rangle_{r\in C_n(P)}.$$

In addition,

$$|G_P(\omega)|^2 \;=\; \left\langle e^{i\omega\cdot(r-q)}\right\rangle_{r,q\in C_n(P)}.$$

It is likewise instructive simply to insert such functions as $f(r) := e^{i\omega\cdot r}$ into the expectation Definition 4.

As we shall see in the next section, there are certain special cases for which the spectral kernel associated with an SCS can be reduced to a product of simpler kernels. In particular, both ${}_nG_n$ and ${}_nG_0$ factor into a n-fold product of 1-dimensional kernels (see Example 5).

Example 3. The 2-dimensional Cantor Dust $C_2(0)$ has an associated spectral kernel which can be factored as

$${}_2G_0(\omega_1,\omega_2) \;=\; {}_1G_0(\omega_1)\cdot{}_1G_0(\omega_2)$$

and so

$$\left\langle e^{i\omega\cdot(r-\mathbf{1/2})}\right\rangle_{r\in C_2(0)} \;=\; \left\langle e^{i\omega_1\cdot(x-1/2)}\right\rangle_{x\in C_1(0)}\left\langle e^{i\omega_2\cdot(x-1/2)}\right\rangle_{x\in C_1(0)}$$

Similarly, the 3-dimensional Cantor Dust $C_3(0)$ has an associated spectral kernel

$${}_3G_0(\omega_1,\omega_2,\omega_3) \;=\; {}_1G_0(\omega_1)\cdot{}_1G_0(\omega_2)\cdot{}_1G_0(\omega_3)$$

and so the pattern continues.

5 Fundamental fractal relations

Remarkably, many of the exact results we shall derive depend exclusively on self-similarity relations. At the very core of such analysis is the following.

Proposition 3 (Spectral self-similarity). *The spectral kernel for a given SCS in n-dimensions with string P satisfies*

$$G_P(\omega) \;=\; S_P(\omega)\, G_P(\omega/3^p),$$

where p is the period of the generating string P, with the similarity factor $S_P = {}_nS_P$ given by the finite product

$$S_P(\omega) := \prod_{k=1}^{p} \frac{1}{N_k} \sum_{Z(b_k)\le P_k} e^{i\omega\cdot b_k/3^k} \tag{20}$$

$$= \prod_{k=1}^{p} \frac{1}{N_k} \sum_{Z(b_k)\le P_k} \cos(\omega\cdot b_k/3^k). \tag{21}$$

It is fairly easy to compute ${}_nS_P$ symbolically. We look at the one dimensional case in more detail in the following section.

Example 4 Similarity relations in two and three dimensions. We have

$$
\begin{aligned}
{}_1S_0(\omega_1) &= \cos\left(\frac{1}{3}\omega_1\right) \\
{}_2S_0(\omega_1,\omega_2) &= {}_1S_0(\omega_1){}_1S_0(\omega_2) \\
{}_2S_1(\omega_1,\omega_2) &= \frac{1}{4}\left({}_1S_0(\omega_1) + {}_1S_0(\omega_2) + 2{}_2S_0(\omega_1,\omega_2)\right) \\
{}_2S_2(\omega_1,\omega_2) &= {}_1S_1(\omega_1){}_1S_1(\omega_2) \\
{}_3S_0(\omega_1,\omega_2,\omega_3) &= {}_1S_0(\omega_1){}_1S_0(\omega_2){}_1S_0(\omega_3) \\
{}_3S_1(\omega_1,\omega_2,\omega_3) &= \frac{1}{5}\left({}_2S_0(\omega_1,\omega_2) + {}_2S_0(\omega_1,\omega_3) + {}_2S_0(\omega_2,\omega_3) + 2{}_3S_0(\omega_1,\omega_2,\omega_3)\right) \\
{}_3S_2(\omega_1,\omega_2,\omega_3) &= \frac{1}{13}\left({}_1S_0(\omega_1) + {}_1S_0(\omega_2) + {}_1S_0(\omega_3)\right. \\
&\qquad \left. +2{}_2S_0(\omega_1,\omega_2) + 2{}_2S_0(\omega_1,\omega_3) + 2{}_2S_0(\omega_2,\omega_3) + 4{}_3S_0(\omega_1,\omega_2,\omega_3)\right) \\
{}_3S_3(\omega_1,\omega_2,\omega_3) &= {}_1S_1(\omega_1){}_1S_1(\omega_2){}_1S_1(\omega_3)
\end{aligned}
$$

as illustrative of the structure of all similarity relations for SCSs. ◇

Example 5 (Similarity relations for period-1 strings in arbitrary dimension n).

$$
{}_nS_0(\omega_1,\omega_2,\ldots,\omega_n) = \prod_{k=1}^{n} {}_1S_0(\omega_k)
$$

$$
{}_nS_n(\omega_1,\omega_2,\ldots,\omega_n) = \prod_{k=1}^{n} {}_1S_1(\omega_k)
$$

and there is more to say as we shall see in Section 8.4. ◇

Such self-similarity triggers a cascade of results attendant on fractal theory. Using the S-factor to rescale integral representations such as (18, 19) yields

Proposition 4 (Scaling relations). *For r, q in R^n, the probability densities, respectively pertaining to the box integrals B, Γ and Δ, satisfy the scaling relations:*

$$\phi(r) = \frac{3^{pn}}{\prod_{k=1}^{p} N_k} \sum_{U(c_k)\leq P_k} \phi(3^p(r - c_1/3 - c_2/3^2 - \cdots - c_p/3^p)) \tag{22}$$

$$\phi(d := r - \mathbf{1/2}) = \frac{3^{pn}}{\prod_{k=1}^{p} N_k} \sum_{Z(b_k)\leq P_k} \phi(3^p(d - b_1/3 - b_2/3^2 - \cdots - b_p/3^p)) \tag{23}$$

$$\Phi(d := r - q) = \frac{3^{pn}}{\prod_{k=1}^{p} N_k^2} \sum_{Z(b_k),Z(a_k)\leq P_k} \Phi(3^p(d - (b_1 - a_1)/3 - \cdots - (b_p - a_p)/3^p)). \tag{24}$$

Finally, we arrive at a functional relation for general expectations; by substitution of the Proposition (4) formulae into expectation integrals such as (14) we achieve:

Proposition 5 (Functional equations for expectations). *For r, q in R^n, and appropriate F we have:*

$$\langle F(r)\rangle_{r\in C_n(P)} = \frac{1}{\prod_{j=1}^{p} N_j} \sum_{U(c_k)\le P_k} \langle F(r/3^p + c_1/3 + \cdots + c_p/3^p)\rangle \tag{25}$$

$$\langle F(d := r - \mathbf{1/2})\rangle_{r\in C_n(P)} = \frac{1}{\prod_{j=1}^{p} N_j} \sum_{Z(b_k)\le P_k} \langle F(d/3^p + b_1/3 + \cdots + b_p/3^p)\rangle \tag{26}$$

$$\langle F(d := r - q)\rangle_{r,q\in C_n(P)} = \frac{1}{\prod_{j=1}^{p} N_j^2} \sum_{Z(b_k),Z(a_k)\le P_k} \langle F(d/3^p + (b_1 - a_1)/3 + \cdots + (b_p - a_p)/3^p)\rangle \tag{27}$$

It is typical of such functional equations—at least in one dimension—that any solution is either absolutely continuous or is singular with respect to Lebesgue measure, see [8] or [7, Chapter 2].

Remark 4. We shall see at the end of the next section that Proposition 3 allows us to show that $G_P(\omega)$ is everywhere convergent as a product. That is, the product is finite and vanishes only if one of the ${}_nS_P(\omega)$ terms does. ◇

6 Exact analyses in $n = 1$ dimension

There are but two possible SCS with period $p = 1$ for embedding dimension $n = 1$; namely $C_1(0)$ (the standard middle-thirds Cantor set) and $C_1(1)$ (the full interval $[0, 1]$).

6.1 The case of $C_1(1)$

From our results on self-similarity we have, for the SCS $C_1(1) = [0, 1]$, that

$$ {}_1G_1(\omega) \;=\; \prod_{k\geq 1} \frac{1}{3}\left(1 + e^{i\omega/3^k} + e^{-i\omega/3^k}\right) $$

This expression is reducible by the following lemma in which we use $\mathrm{sinc}(x) := \sin(x)/x$:

Lemma 1. *For all ω in R we have*

$$ {}_1G_1(\omega) = \prod_{k\geq 1} \frac{1}{3}\left(1 + e^{i\omega/3^k} + e^{-i\omega/3^k}\right) = \mathrm{sinc}\left(\frac{\omega}{2}\right). \tag{28} $$

Proof. Note as above, that $e^{i\omega/3^k} + e^{-i\omega/3^k} = 2\cos(\omega/3^k)$. Define the function:

$$Q(x) := x \prod_{k\geq 1} \frac{1}{3}\left(1 + 2\cos(2x/3^k)\right).$$

Then Lemma 1 is equivalent, via the change-of-variables $x = \omega/2$, to the statement: $Q(x) = \sin(x)$. Now,

$$\begin{aligned}
\frac{Q(3x)}{Q(x)} &= \frac{3x\prod_{k\geq 1}\frac{1}{3}\left(1+2\cos(2x/3^{k-1})\right)}{x\prod_{k\geq 1}\frac{1}{3}\left(1+2\cos(2x/3^k)\right)} = 3\prod_{k\geq 1}\left(\frac{1+2\cos(2x/3^{k-1})}{1+2\cos(2x/3^k)}\right) \\
&= 3\left(\frac{1+2\cos(2x)}{1+2\cos(2x/3)}\right)\left(\frac{1+2\cos(2x/3)}{1+2\cos(2x/3^2)}\right)\cdots \\
&= 3\left(\frac{1+2\cos(2x)}{1+2\cos(0)}\right) = 1+2\cos(2x) = \frac{\sin(3x)}{\sin(x)}
\end{aligned}$$

and by recursion,

$$\frac{Q(x)}{\sin(x)} = \frac{Q(x/3)}{\sin(x/3)} = \frac{Q(x/9)}{\sin(x/9)} = \cdots$$

Therefore,

$$\begin{aligned}
\frac{Q(x)}{\sin(x)} &= \lim_{x\to 0}\frac{Q(x)}{\sin(x)} \\
&= \lim_{x\to 0}\frac{1}{x}\cdot x\prod_{k\geq 1}\frac{1}{3}\left(1+2\cos(2x/3^k)\right) \\
&= \lim_{x\to 0}\prod_{k\geq 1}\left(1-\frac{4}{3}\sin^2(x/3^k)\right) = 1
\end{aligned}$$

since the final product is absolutely convergent and is continuous at zero. □

Returning to the SCS $C_1(1) = [0,1]$ with ${}_1G_1(\omega) = \operatorname{sinc}(\omega/2)$, we see that this special case (of fractal dimension 1) has probability density

$$\phi(r) = 1/(2\pi) \int e^{-i\omega(r-1/2)} {}_1G_1(\omega) \mathrm{d}\omega$$

which is a "square pedestal" situated on $[0,1]$, as expected—that is the transform of *sinc* (which is only conditionally convergent) is the characteristic function of the interval.

Example 6 (The easiest classical box integral). Likewise, continuing to imaginary $\omega = it$, we have an expectation for parameter t:

$$\left\langle e^{-tr} \right\rangle_{r\in[0,1]} = \frac{1-e^{-t}}{t},$$

giving in turn the (trivially known) box integral

$$B(s, C_1(1)) = B_1(s) = \frac{1}{s+1}. \tag{29}$$

When $s \geq 0$ is integer, this follows from the series for $(1-e^{-t})/t$. When s is non-integer, consider the region $\Re(s) \in (-1,0)$, where

$$\langle r^s \rangle = \frac{1}{\Gamma(-s)} \int_0^\infty t^{-s-1} \langle e^{-rt} \rangle \, \mathrm{d}t$$

$$= \frac{1}{\Gamma(-s)} \int_0^\infty t^{-s-2} (1-e^{-t}) \, \mathrm{d}t = \frac{1}{s+1}.$$

We may then infer (29) by analytic continuation on appealing to analyticity of the box representation as discussed at the end of §3.1. ◇

The scaling relation for this SCS is also instructive. We have $N_1 = 3$ admissible ternary digits, so from Proposition 4 we have

$$\phi(r) \;=\; \phi(3r) + \phi(3r-1) + \phi(3r-2),$$

which (almost everywhere) admits the unit pedestal solution.

But perhaps most interesting in this simple case is the two-point density $\Phi(d := r - q)$, with scaling relation for $r, q \in [0, 1]$:

$$\Phi(d) \;=\; \frac{1}{3}\,(3\,\Phi(3d) + 2\,\Phi(3d-1) + 2\,\Phi(3d+1) + \Phi(3d+2) + \Phi(3d-2))$$

Indeed, this relation is satisfied a.e. by the "unit tent," with a graph of Φ being a triangle with base $[-1, 1]$ and apex at $(0, 1)$ and likewise for the appropriate density for the difference $d = r - q$.

6.2 The case of $C_1(0)$

As one would expect, the above discussion for the degenerate case $C_1(1) = [0, 1]$ only becomes more complicated as the defining string is modified. For the standard Cantor set $C_1(0)$ we have the scaling relation

$$\phi(r) \;=\; \frac{3}{2}(\phi(3r) + \phi(3r-2)),$$

which is satisfied a.e. in the sense of distribution theory.[7] However, one may often *integrate* over such pathological densities with impunity. The spectral kernel as defined in (16) now becomes:

$$ {}_1G_0(\omega) = \prod_{k\geq 1} \cos(\omega/3^k), \tag{30}$$

from which we develop generating-function relations, starting with:

$$ \sum_{m\geq 0} B(m, C_1(0)) \frac{t^m}{m!} \;=\; \left\langle e^{tr} \right\rangle_{r\in C_1(0)} \;=\; e^{t/2} \prod_{k\geq 1} \cosh(t/3^k). \tag{31}$$

Now a simple scaling $t \to 3t$ results in another series

$$ \begin{aligned} \sum_{k\geq 0} B(k, C_1(0)) \frac{3^k t^k}{k!} \;&=\; \left\langle e^{3tr} \right\rangle_{r\in C_1(0)} \;=\; e^{3t/2} \cosh t \prod_{k\geq 1} \cosh(t/3^k) \\ &=\; e^t \cosh t \sum_{m\geq 0} B(m, C_1(0)) \frac{t^m}{m!}. \end{aligned} \tag{32}$$

Matching the coefficients of powers of t for the far left and far right series in (32) immediately resolves *all* box integrals $B(m, C_1(0))$ for nonnegative integers m. Note importantly that both Theorem 2 and the Δ-counterpart theorem following can alternatively be established via self-similarity relations starting with (42), without direct recourse to series algebra:

Theorem 2. **[Closed form for certain** $B(s, C_1(0))$**]** *For any non-negative integer* m*, the expectation* $\langle |r|^m \rangle$ *for* r *in the standard Cantor set* $C_1(0)$ *is given exactly by the recursion, ignited by* $B(0, C_1(0)) = 1$*, for* $m \geq 1$*,*

$$ B(m, C_1(0)) \;=\; \frac{1}{3^m - 1} \sum_{j=0}^{m-1} \binom{m}{j} 2^{m-j-1} B(j, C_1(0)). \tag{33}$$

[7] Recall this ϕ is nonzero only on the Cantor set—and yet should have measure one, so it belongs to the world of delta-functions and their generalizations (or of singular measures).

Let us illustrate as follows:

Example 7. The first eight values of the box integral B over $C_1(0)$ are thus:

$$\{B(0, C_1(0)), B(1, C_1(0)), \dots, B(7, C_1(0)), \dots\} \;=\; \left\{1, \frac{1}{2}, \frac{3}{8}, \frac{5}{16}, \frac{87}{320}, \frac{31}{128}, \frac{10215}{46592}, \frac{2675}{13312}, \dots\right\},$$

and so on. ◇

A very similar argument—this time involving the square of ${}_1G_0(\omega)$, yields a companion result for any separation moment $\Delta(m, C_1(0))$ for $m = 0, 1, 2, 3, \dots$:

Theorem 3. [Closed form for certain $\Delta(s, C_1(0)$] *For any non-negative integer m, the expectation $\langle |r - q|^m \rangle$ for r, q in the standard Cantor set $C_1(0)$ is given exactly by the ignition $\Delta(0, C_1(0)) := 1$ and the recursion*

$$\Delta(m, C_1(0)) \;=\; \frac{2^m}{2 \cdot 3^m - 2 + (m \bmod 2)} \sum_{k=0}^{\lfloor (m-1)/2 \rfloor} \binom{m}{2k} 4^{-k}\, \Delta(2k, C_1(0)). \tag{34}$$

Again we illustrate :

Example 8. The first eight values of the box integral Δ over $C_1(0)$ are thus:

$$\{\Delta(0, C_1(0)), \Delta(1, C_1(0)), \dots, \Delta(7, C_1(0)), \dots\} \;=\; \left\{1, \frac{2}{5}, \frac{1}{4}, \frac{19}{106}, \frac{11}{80}, \frac{427}{3880}, \frac{529}{5824}, \frac{139681}{1819168}, \dots\right\},$$

and so on. ◇

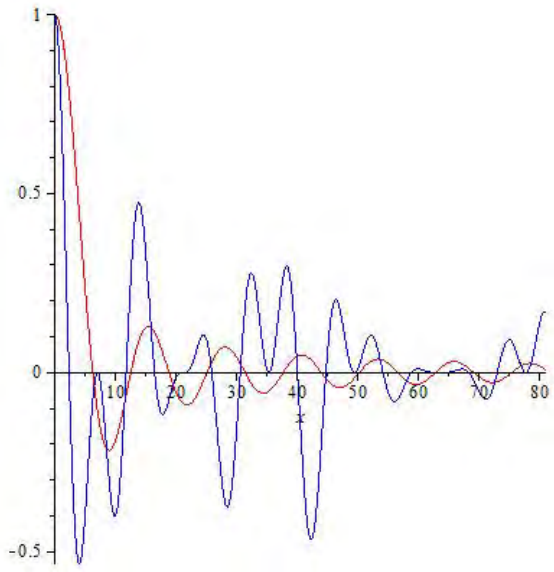

Figure 3: The sinc function ${}_1G_1(\omega)$ (28) and the more oscillatory ${}_1G_0(\omega)$ (30).

Theorems 2 and 3 immediately imply the following striking result:

Corollary 1. *For any non-negative integer s, both the box integrals $B(s, C_1(0))$ and $\Delta(s, C_1(0))$ are rational.*

The complexity of ${}_nG_P$ is illustrated in Figure 6.2 just for $n = 1$. It is also instructive to compute and plot ${}_1G_{01}$ and ${}_1G_{10}$ which share their fractal dimension but not their moments (see Appendix A1). Note that

$$ {}_1S_{01}(\omega_1) = \frac{1}{3}\left(\cos\left(2/9\,\omega_1\right) + \cos\left(3/9\,\omega_1\right) + \cos\left(4/9\,\omega_1\right)\right), $$

and

$$ {}_1S_{10}(\omega_1) = \frac{1}{3}\left(\cos\left(1/9\,\omega_1\right) + \cos\left(2/9\,\omega_1\right) + \cos\left(4/9\,\omega_1\right)\right), $$

while

$$ {}_2S_{20}(\omega_1, \omega_2) =_1 S_{10}(\omega_1) \cdot_1 S_{10}(\omega_2). $$

6.3 Estimation of ${}_nG_P$

We conclude this section with simple estimates of the size of $G_P(\omega)$ for arbitrary P of period length p and any n. We first observe that

$$ {}_nG_P(\omega) = \prod_{m=1}^{\infty} {}_nS_p\left(\frac{\omega}{3^{mp}}\right) \tag{35}$$

where

$$ {}_nS_P(\omega) = \prod_{k=1}^{p} \frac{1}{N_k} \sum_{Z(b_k)\le P_k} \cos\left(\frac{\omega\cdot b_k}{3^k}\right) \tag{36}$$

is as given by (21) of Proposition 3. Fix ω and select m_0 so $|\omega/3^{mp}| \le \pi/2$ for $m \ge m_0$. Since (36) represents ${}_nS_P(\omega/3^{mp})$ as a product of weighted arithmetic means of cosine values with domain $[-\pi/2, \pi/2]$ each term exceeds $\cos(\|\omega\|_1/3^{mp+k})$ and is at most 1 we deduce

$$\begin{aligned} \prod_{m=1}^{m_0-1}\left|{}_nS_p\left(\frac{\omega}{3^{mp}}\right)\right| \ge |{}_nG_P(\omega)| &\ge \prod_{m=1}^{m_0-1}\left|{}_nS_p\left(\frac{\omega}{3^{mp}}\right)\right| \prod_{m=m_0}^{\infty}\prod_{k=1}^{p}\cos\left(\frac{\|\omega\|_1}{3^{mp+k}}\right) \\ &= \prod_{m=1}^{m_0-1}\left|{}_nS_p\left(\frac{\omega}{3^{mp}}\right)\right| \prod_{i=m_0}^{\infty}\cos\left(\frac{\|\omega\|_1}{3^{i}}\right). \end{aligned} \tag{37}$$

From (37) and Lemma 1 we deduce:

Lemma 2. *For all ω in R^n we have*

$$ \prod_{m<m_0}\left|{}_nS_p\left(\frac{\omega}{3^{mp}}\right)\right| \ge |{}_nG_P(\omega)| \ge \prod_{m<m_0}\frac{\left|{}_nS_p\left(\frac{\omega}{3^{mp}}\right)\right|}{\left|\cos\left(\frac{\|\omega\|_1}{3^m}\right)\right|}\cdot {}_1G_0(\|\omega\|_1). \tag{38}$$

In particular, the kernel ${}_nG_P(\omega) = \prod_{m=1}^{\infty} {}_nS_p(\omega/3^{pm})$ is an everywhere convergent product which can vanish only at zeros of ${}_nS_p$ or of cosine.

In (38) we note that the denominator on the right can only vanish when ${}_1G_1$ does and so the apparent singularities disappear.

7 Second moments for a general SCS

The functional expectation relations of Proposition 5 can be used directly to yield all expectations $B(2, C_n(P))$ as rational numbers depending only on the defining string P and embedding dimension n, as follows:

Theorem 4 (Closed form for $B(2, C_n(P))$). *For any embedding dimension n and SCS $C_n(P)$ the box integral $B(2, C_n(P))$ is rational, given by the closed form:*

$$B(2, C_n(P)) \;=\; \frac{n}{4} + \frac{1}{1-9^{-p}} \sum_{k=1}^{p} \frac{1}{9^k} \frac{\sum_{j=0}^{P_k} \binom{n}{j} 2^{n-j} (n-j)}{\sum_{j=0}^{P_k} \binom{n}{j} 2^{n-j}}, \tag{39}$$

and the corresponding box integral $\Delta(2, C_n(P))$ is also rational, given by:

$$\Delta(2, C_n(P)) \;=\; 2B(2, C_n(P)) - \frac{n}{2}. \tag{40}$$

Proof. For (39), take $F(r) := |r|^2$ in Proposition 5, so that for $d := r - \mathbf{1/2}$ the expectation $\langle d \cdot d \rangle$ is proportional to a sum of expectations

$$\langle (d/3^p + b_1/3 + \cdots + b_p/3^p)^2 \rangle.$$

Observe that expectations of dot-products $b_j \cdot b_k$ all vanish (this is how the second-moment problem especially simplifies), and one is left with a simpe if tedious combinatorial end-argument for this sum of b_k-dependent expectations.

For (40), we argue as follows. We have, simply, for vectors r, q each ranging over the given SCS,

$$\begin{aligned} \Delta(2, C_n(P)) &= \left\langle |r-q|^2 \right\rangle \\ &= \left\langle r^2 \right\rangle + \left\langle q^2 \right\rangle - 2 \langle r \cdot q \rangle \\ &= 2B(2, C_n(P)) - 2 \langle r \cdot q \rangle . \end{aligned}$$

Now there is a trick to evaluate the dot-product expectation, namely write

$$(r - \mathbf{1/2}) \cdot (q - \mathbf{1/2}) = 0,$$

by symmetry of any SCS around the centroid vector $\mathbf{1/2}$. Expanding out this vanishing expectation, we find $\langle r \cdot q \rangle = n/4$, which proves the Δ relation of the theorem. □

Example 9. The first few cases of Theorem 4 for period-1 strings P are:

$$\begin{aligned} B(2, C_n(0)) &= \frac{3}{8}n, \\ B(2, C_n(1)) &= \frac{n(3n+5)}{8n+16}, \\ B(2, C_n(2)) &= \frac{n(3n^2+7n+22)}{8n^2+24n+64}, \\ B(2, C_n(n-1)) &= \frac{n}{4}\left(1 + \frac{3^{n-1}}{3^n-1}\right), \end{aligned}$$

together with:

$$\begin{aligned} \Delta(2, C_n(0)) &= \frac{1}{4}n, \\ \Delta(2, C_n(1)) &= \frac{n(n+1)}{4n+8}, \\ \Delta(2, C_n(2)) &= \frac{n(n^2+n+6)}{4n^2+12n+32}, \\ \Delta(2, C_n(n-1)) &= \frac{n}{6}\left(\frac{3^n}{3^n-1}\right), \end{aligned}$$

Note for comparison that the classical box integrals over the unit n-cube are:

$$B_n(2) = \frac{n}{3} \quad \text{and} \quad \Delta_n(2) = \frac{n}{6} \tag{41}$$

which matches the output of Theorem 4 for $P = n$. ◇

Exact rational values for various strings in dimensions 1, 2 and 3 are shown in appendix 1. Computational data derived from Proposition and Theorem 4 concerning the relationship between fractal dimension and the box integrals $B(2, C_n(P))$ and $\Delta(2, C_n(P))$ is shown in tabulated values and scatterplots in the appendix. These scatterplots show a great deal of fractal structure in and of themselves.

Remark 5. An empirical example of ordering of box-integral values is the amusing pair:

$$B_3(2) \;=\; 1, \text{ but } B(2, C_3(2)) \;=\; \frac{105}{104}.$$

This kind of observation that provokes thoughts of a monotonicity-ordering principle. One might hypothesise that any two SCSs $C_n(P)$ and $C_n(P')$ will satisfy

$$\delta(C_n(P)) \geq \delta(C_n(P')) \;\stackrel{?}{\Longrightarrow}\; B(s, C_n(P)) \leq B(s, C_n(P')),$$

and similarly for $\Delta(s, C_n(P))$. However, our computational experiments show that no such ordering principle exists. For instance, in embedding dimension $n = 1$,

$$\begin{aligned} \delta(C_1(100)) &= 0.75\ldots \\ \delta(C_1(01)) &= 0.81\ldots \end{aligned}$$

while,

$$\begin{aligned} B(C_1(100)) &= \frac{123}{364} = 0.33\ldots \\ B(C_1(01)) &= \frac{89}{240} = 0.37\ldots \end{aligned}$$

Appendix A holds more computational data regarding the second separation moments of SCSs. ◇

8 Self-similarity and analyticity

What can be said about integrals $B(s, C_n(P))$ in general? Certainly the relative ease of analysis for a simple string P or moment $s = 2$ will not carry over generally. For one thing, the classical box integrals $B_n(s)$—which are as our fractal cases for $C_n(n) = [0,1]^n$—are currently unknown in closed form past $n = 5$, see [9]. Nonetheless, one may still exploit self-similarity for general s.

For example, it follows from Proposition 5 that for the standard middle-thirds Cantor set:

$$B(s, C_1(0)) \;:=\; \langle |r^s| \rangle_{r \in C_1(0)} = \frac{1}{2} \left\langle \left(\frac{r}{3}\right)^s \right\rangle + \frac{1}{2} \left\langle \left(\frac{r+2}{3}\right)^s \right\rangle , \tag{42}$$

$$\Delta(s, C_1(0)) \;:=\; \langle |d := r - q|^s \rangle = \frac{1}{2}\frac{1}{3^s} \langle |d|^s \rangle \;+\; \frac{1}{4}\frac{1}{3^s} \langle (2+d)^s + (2-d)^s \rangle . \tag{43}$$

These are powerful self-similarity relations, yielding both theoretical knowledge and exact expressions for certain values of s. An immediate result emerges when we write, say, an equivalent form of (42), using the fact that the first expectation, that of $(r/3)^s$, is a scaled box integral itself, leading to

$$B(s, C_1(0)) = \frac{1}{2 \cdot 3^s - 1} \langle (r+2)^s \rangle . \tag{44}$$

8.1 Pole theorem

This last expression (44) reveals a pole in the s-plane, namely at $s = -\log_3 2$. It is not a coincidence that the pole location is the negated fractal dimension. Indeed, self-similarity implies a general result:

Theorem 5. [Poles of $B(s, C_n(P))$] *For any embedding dimension n and any SCS $C_n(P)$, the (analytically continued) box integral $B(s, C_n(P))$ has a pole at*

$$s = -\delta(C_n(P)). \tag{45}$$

Proof. The functional relations of Proposition 5 let us write

$$B(s, C_n(P)) := \langle |r|^s \rangle_{r \in C_n(P)} = \frac{1}{\prod_{j=1}^{p} N_j} \sum_{U(c_k) \le P_k} |r/3^p + c_1/3 + \cdots + c_p/3^p|^s$$

$$= \frac{1}{\prod_{j=1}^{p} N_j} 3^{-ps} B(s, C_n(P)) + \frac{1}{\prod_{j=1}^{p} N_j} {\sum_{U(c_k) \le P_k}}' |r/3^p + c_1/3 + \cdots + c_p/3^p|^s,$$

where the last, primed sum indicates—importantly—that not all $U(c_k)$ can be 0 in the sum. But said primed sum is always finite for any s, as it is sum of expectations of $|ar + b|^s$ with $a, b > 0$.

Now on regrouping we have

$$\left(1 - \frac{3^{-ps}}{\prod_j N_j}\right) B(s, C_n(P)) = \frac{1}{\prod_{j=1}^{p} N_j} {\sum_{U(c_k) \le P_k}}' |r/3^p + c_1/3 + \cdots + c_p/3^p|^s, \tag{46}$$

Now the companion factor to B in (46), namely $(1 - 3^{-ps}/\prod_j N_j)$ vanishes at the fractal dimension $s = -\delta(C_n)$ (given in Proposition 7) while the right side remains bounded away from zero. It follows that B must have a pole at such s. □

Note the attractive corollary that for the full n-cube $[0, 1]^n$, the pole is at $s = -n$, consistent with the classical theory.

Remark 6. We have been unable as yet to develop pole structure for integrals $\Delta(s, C_n)$, arbitrary n. For one thing, the literature on classical box integrals states that $\Delta_n(s)$ always has $(n + 1)$ complex poles, unlike $B_n(s)$ which always has one. And yet, we have seen no evidence that multiple poles accrue for any SCS of fractal dimension $< n$ in embedding dimension n. ◇

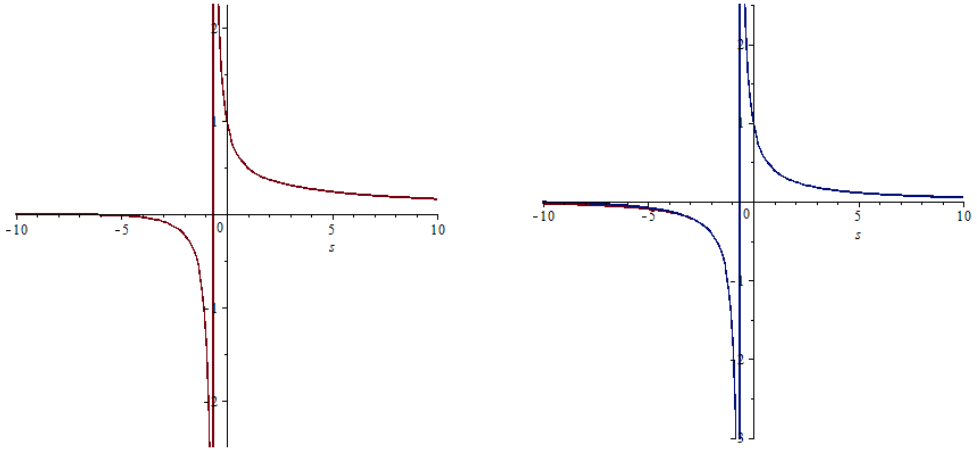

Figure 4: $B(s, C_1(0))$ and $\Delta(s, C_1(0))$ drawn from (47).

8.2 Fractal-box series

Relation (44) also allows us to expand the expectation bracket to obtain an analytic series in s for the Cantor case $C := C_1(0)$:

$$B(s,C) \;=\; \frac{2^s}{2\cdot 3^s-1}\sum_{j\geq 0}\binom{s}{j}\frac{1}{2^j}B(j,C), \tag{47}$$

where—remarkably enough—we know *every* $B(j,C)$ via Theorem 2. (We made use (47) for $s \neq 0,1,2,3,\ldots$, having precomputed a sufficiently wide set of $B(j,.)$ values from said Theorem.) As for a Δ-series again for $C := C_1(0)$, we may use (43) similarly to develop

$$\Delta(s,C) \;=\; \frac{2^s}{2\cdot 3^s-1}\sum_{\text{even } j\geq 0}\binom{s}{j}\frac{1}{2^j}\Delta(j,C), \tag{48}$$

and knowledge of $\Delta(j,C)$ for $j = 0,1,2,3,\ldots$ gives rise to a fine numerical series.

It seemed to us natural to look at such expansions and infer asymptotic behavior for large s. Numerical experiments are embodied in accurate B-plots of Figure 5, and made good use of the fractal-box series (47); all of this leading us to

Conjecture 1 (**Asymptotics**). *Let* $\delta := \log_3 2$*, the fractal dimension of* $C_1(0)$*.*

1. *For large* s *we have*

$$B(s, C_1(0)) \sim \frac{A}{s^\delta},$$

where $A \approx 0.7$ *is an absolute constant.*

2. *Similarly,*

$$\Delta(s, C_1(0)) \sim \frac{A'}{s^{2\delta}},$$

where the absolute constant $A' \approx 1.07$*.*

Remark 7. Conjecture 1 seems reasonable, on the very loose heuristic that if, in the sum (47) we have $B_j \sim A/j^\delta$, then a complicated integral-approximation argument gives the left-hand side $\sim A/s^\delta$. We have left out the heuristic argument, but we do emphasize the conjecture. The corresponding conjecture for $\Delta(s, C_1(0))$, follows from the numerical observation that $2B(s, C_1(0))^2/\Delta(s, C_1(0))$ appears to tend to a limit of approximately 0.73 for large real $|s|$. ◇

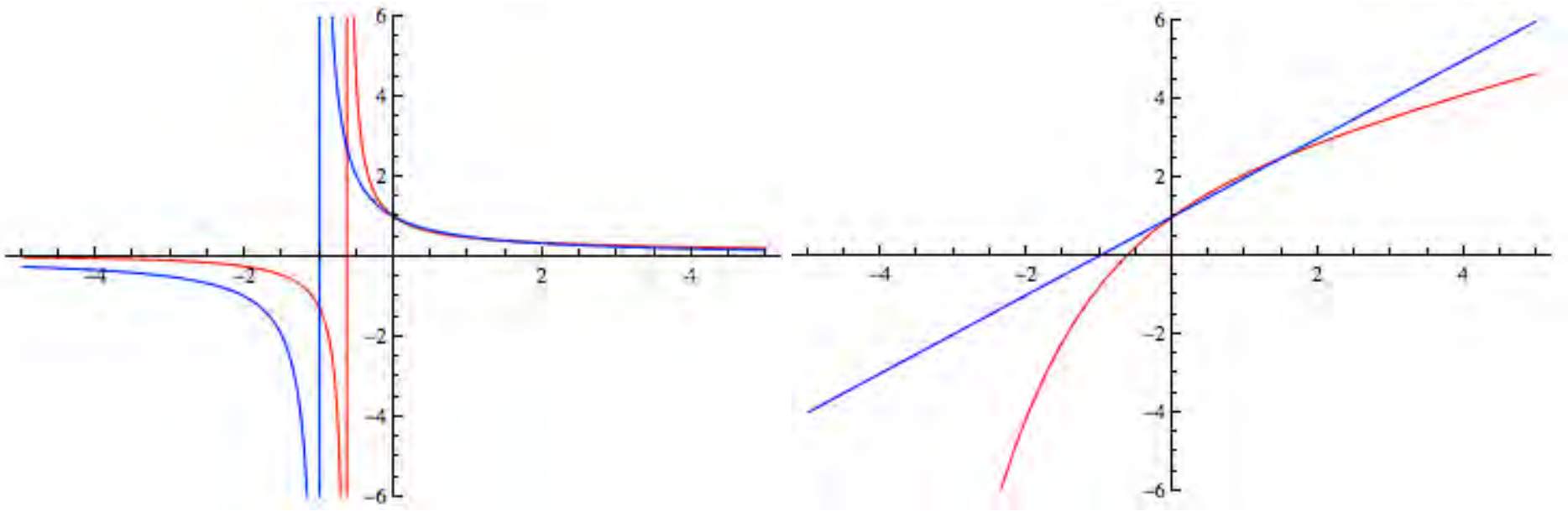

(a) $B(s, C_1(1))$ and $B(s, C_1(0))$

(b) Reciprocals of $B(s, C_1(1))$ and $B(s, C_1(0))$

Figure 5: Analytic plots of box integrals for real s. Figure 5(a) shows $B_1(s) = B(s, C_1(1)) = 1/(s+1)$ (with a pole at $s = -1$) and $B(s, C_1(0))$ (with a proven pole at $s = -\log_3 2$). Figure 5(b) plots reciprocals: a perfectly straight line $\sim s$ itself and $1/B(s, C_1(0)) \sim s^{\log_3 2}$ for large s (unproven).

8.3 High-precision algorithm for general B

We next exhibit a novel algorithm that allows not only high-precision expectations,[8] but also *rigorous* bounds on such expectations. Note first the principle—immediately following from the SCS definition—that we have set equality

$$C_n(P) \;=\; C_n(P \cdot P \cdots P),$$

[8] Meaning, say, 20 digits. In previous works we have used the phrase "extreme precision" to mean at least 100 digits, or certainly enough to discover identities via integer-relation detection.

where $P \cdot P \cdots P$ is any finite string of copies of P. This trivial observation gives rise to a powerful computational expedient. We first recast (46) as

$$\left(3^{pqs}\prod_{j=1}^{p} N_j^q - 1\right) B(s, C_n(P)) \;=\; {\sum_{U(c_k)\le P_k}}' \langle |r + c_{p+1}3^{p'-p-1} + \cdots + c_{p'}|^s\rangle \;+ \tag{49}$$
$$\sum_{\substack{U(c_k)\le P_k \\ (c_1,\ldots c_p)\neq(\mathbf{0}_n,\ldots,\mathbf{0}_n)}} \langle |r + c_1 3^{p'-1} + c_2 3^{p'-2} + \cdots + c_{p'}|^s\rangle,$$

where now the sequence (P_k) is interpreted as having period $p' := pq$. The whole point of these manipulations is that freedom of choice on q allows arbitrarily large powers of 3 within the expectation terms on the right. Remarkably, what we have gained from (49) is the ability to recurse on the multiplicity factor q. Indeed, the primed-sum in (49) is—up to a constant factor—a representation for the same B but involving $(q-1)$ copies. Putting this all together, we arrive at

$$B(s, C_n(P)) \;=\; \frac{1}{Q(s,q,P)} \sum_{\substack{U(c_k)\le P_k \\ (c_1,\ldots c_p)\neq(\mathbf{0}_n,\ldots,\mathbf{0}_n)}} \langle |r + c_1 3^{p'-1} + c_2 3^{p'-2} + \cdots + c_{p'}|^s\rangle, \tag{50}$$

where

$$Q(s,q,P) \;:= 3^{ps(q-1)} \prod_{j=1}^{p} N_j^{q-1} \left(3^{ps}\prod_{j=1}^{p} N_j \;-\; 1\right).$$

The fact that relation (50) is valid for every multiplicity factor $q = 1, 2, 3, \ldots$ leads us to

Algorithm 1 (**High-precision B computation with rigorous bounds**). Given an SCS $C_n(P)$ and a complex power s, the algorithm returns a precise value for $B(s, C_n(P))$, and—if desired, and for suitable s—rigorous bounds on B.

1. For increasing q, calculate B from $B(s, C_n(P))$

$$= \lim_{q\to\infty} \frac{1}{Q(s,q,P)} \sum_{\substack{U(c_k)\le P_k \\ (c_1,\ldots c_p)\neq(\mathbf{0}_n,\ldots,\mathbf{0}_n)}} |(\mathbf{1/2})_n + c_1 3^{p'-1} + c_2 3^{p'-2} + \cdots + c_{p'}|^s, \tag{51}$$

where $p' := pq$, and we have fixed r to be the centroid of the unit n-cube $[0,1]^n$, so expectation brackets have been removed.[9]

2. These B approximations for increasing q will approach the true B value, usually smoothly enough that Aitken (or other) extrapolation will significantly increase accuracy.

3. For rigorous bounds, observe that every component of every vector appearing within the expectation brackets in (49) is nonnegative, so that for real nonnegative s we may consider r to be either the origin $\mathbf{0}_n$ or the far apex $\mathbf{1}_n$ of the unit n-cube, to deduce

$$\frac{1}{Q(s,q,P)} \sum_{\substack{U(c_k)\le P_k \\ (c_1,\ldots c_p)\neq(\mathbf{0}_n,\ldots,\mathbf{0}_n)}} |\mathbf{0}_n + c_1 3^{p'-1} + c_2 3^{p'-2} + \cdots + c_{p'}|^s$$

$$\le \quad B(s, C_n(P)) \quad \le$$

$$\frac{1}{Q(s,q,P)} \sum_{\substack{U(c_k)\le P_k \\ (c_1,\ldots c_p)\neq(\mathbf{0}_n,\ldots,\mathbf{0}_n)}} |\mathbf{1}_n + c_1 3^{p'-1} + c_2 3^{p'-2} + \cdots + c_{p'}|^s.$$

Numerical examples of this algorithm in action are given in Section **??**. □

[9] Certainly this approximation sequence works for $\Re(s) \ge 0$; we conjecture that it works for all complex s, based on numerical trials.

8.4 General monomial moments

We define a monomial moment in terms of an n-vector $m = (m_1, \ldots, m_n)$ of nonnegative integers

$$\mathcal{M}(m, C_n(P)) \;:=\; \langle x_1^{m_1} x_2^{m_2} \cdots x_n^{m_n} \rangle_{x \in C_n(P)} \,.$$

When the SCS $C_n(P)$ is understood, we shall simplify to ${}_n\mathcal{M}(m) = \mathcal{M}(m)$.

First we list some elementary properties of monomial moments $\mathcal{M}$:

1. $\mathcal{M}(m) = \mathcal{M}(m')$ where m' is any coordinate permutation of m. This follows from the symmetry in the definition of an SCS.

2. For any SCS, $\mathcal{M}((1, 0, 0, 0, dots)) = \frac{1}{2}$. Again this follows from symmetry.

3. For any Cantor dust $C_n(0)$, the monomial moments are separable, that is

$$\mathcal{M}(m) \;:=\; \left\langle \prod x_h^{m_h} \right\rangle \;=\; \prod \langle x_h^{m_h} \rangle \,.$$

   This follows in any of several ways. One is to observe that the spectral G kernel separates for $C_n(0)$, so that expectation integrals completely factor. Another is to work through the combinatorics of Theorem 6 below.[10]

4. An immediate generalization is to *difference-monomial moments*. For separation problems involving Δ expectations, we define

$$\mathcal{D}(m) \;:=\; \langle (x_1 - q_1)^{m_1} \cdots (x_n - q_n)^{m_n} \rangle \,,$$

   with elementary properties similar to those above. Only no a coordinate separation variable $x_i - q_i$ is bipolar, running over $[-1, 1]$).

[10] Caveat: we do not know precisely which monomial moments do *not* separate. For example, in 2 dimensions, $\langle xy \rangle = \langle x \rangle \langle y \rangle$ for any SCS, meaning for any of $C_2(0), C_2(1), C_2(2) = [0, 1]^2$.

We now provide a theorem generalizing the explicit results of Theorem 4:

Theorem 6 (**Monomial rationality**). *For any SCS $C_n(P)$, every monomial moment $\mathcal{M}(m)$ is rational, and can be given an explicit closed form. The same properties hold for difference-monomial moments $D(m)$.*

Proof. Now from the first functional relation in Proposition 5 we may use $F(x) := \prod x_h^{m_h}$ to obtain

$$\mathcal{M}(m) \;=\; \frac{1}{\prod_{j=1}^{p} N_j} \sum_{U(c_k)\le P_k} \left\langle \prod_{h=1}^{n} (x_h/3^p + c_{1h}/3 + \cdots + c_{ph}/3^p)^{m_h} \right\rangle, \tag{52}$$

where c_{jh} is the h-th element of column c_j from display (7). Now define the *weight* of a monomial as $W(m) := \sum m_h$, and observe that in this functional relation there are exactly $\prod_{j=1}^{p} N_j$ summands, each having a leading term $\langle \prod (x_h/3^p)^{m_h}$, so that

$$\left(1 - \frac{1}{3^{pW}}\right) \mathcal{M}(m) \;= \sum R(m')\mathcal{M}(m'), \tag{53}$$

where the R coefficients are all rational and m' runs over a set of n-vectors *each of whose weights $W(m')$ being strictly less than $W(m)$*. Therefore one has a multilevel recursion that has to finitely terminate with $\mathcal{M}(m)$ being a rational number. □

Corollary 2 (**Even moment rationality**). *For any SCS $C_n(P)$ and any nonnegative even integer u, both $B(u, C_n(P))$ and $\Delta(u, C_n(P))$ are rational and each can be given an explicit closed form.*

Proof. Everything follows with nonnegative even integer u, from

$$|x|^u \;=\; \left(x_1^2 + \cdots x_n^2\right)^{u/2},$$

whence the right-hand side can be expanded in monomials. □

Example 10 Explicit coefficients. An instance of Corollary 2 is

$$B(4, C_2(1)) \;=\; \langle (x^2+y^2)^2 \rangle \;=\; 2\mathcal{M}((4,0)) + 2\mathcal{M}(2,2) \;=\; \frac{429}{640},$$

while for the dust SCS, we obtain

$$B(4, C_2(0)) \;=\; \frac{33}{40}.$$

Moreover, in the case of n-dimensional Cantor dust we have complete separability of the underlying density (as discussed above for the monomials). Thence, for integers $m > 0$ we obtain from the binomial theorem that

$$B(2m, C_n(0)) = \sum_{\substack{k_1,k_2,\ldots,k_n \geq 0 \\ \sum_j k_j = m}} \binom{m}{k_1, \ldots, k_n} \prod_{j=1}^{n} b_{2k_j} \tag{54}$$

where $b_n := B(n, C_1(0))$ is as given by Theorem 2. ◇

Example 11 Monomial recursion. An example of using the recursion in the proof of Theorem 6 is as follows. A collection of moments $\mathcal{M}((i,j)) = \langle x^i y^j \rangle$ for vectors (x, y) on the SCS $C_2(1)$ is

$$\left\langle \begin{array}{cccc} 1 & y & y^2 & y^3 \\ x & xy & xy^2 & xy^3 \\ x^2 & x^2y & x^2y^2 & x^2y^3 \\ x^3 & x^3y & x^3y^2 & x^3y^3 \end{array} \right\rangle = \begin{pmatrix} 1 & \frac{1}{2} & \frac{11}{32} & \frac{17}{64} \\ \frac{1}{2} & \frac{1}{4} & \frac{11}{64} & \frac{17}{128} \\ \frac{11}{32} & \frac{11}{64} & \frac{601}{5120} & \frac{923}{10240} \\ \frac{17}{64} & \frac{17}{128} & \frac{923}{10240} & \frac{1409}{20480} \end{pmatrix},$$

whereas for the SCS $C_2(0)$, the corresponding matrix of moments is

$$= \begin{pmatrix} 1 & \frac{1}{2} & \frac{3}{8} & \frac{5}{16} \\ \frac{1}{2} & \frac{1}{4} & \frac{3}{16} & \frac{5}{32} \\ \frac{3}{8} & \frac{3}{16} & \frac{9}{64} & \frac{15}{128} \\ \frac{5}{16} & \frac{5}{32} & \frac{15}{128} & \frac{25}{256} \end{pmatrix}.$$

Remarkably, $< xy >= 1/4$ separates as $(1/2) \cdot (1.2)$ for each SCS here, and for $C_2(2) = [0,1]^2$, but some other elements of the matrix for $C_2(1)$ are *not* separable. $\diamond$

9 Numerical algorithms, results and challenges

We have given rational closed $B(s,\cdot), \Delta(s,\cdot)$ forms for all non-negative integer s in $n = 1$ dimension, and for all dimensions n we have proven the existence of rational closed forms when s is even.

Yet, we have no evaluation when $n \geq 2$ and s is not an even integer, say $s = 1, n = 2$ as canonical 'open case.' We do not yet know the expectation of distance from the origin $B(1,\cdot)$, or the expected separation $\Delta(1,\cdot)$, on any non-trivial SCS embedded in $n \geq 2$ dimensions.

Example 12. [**Selected numerical excursions**] We list some of our successes and some of the challenges remaining.

1. An initial numerical foray was that of V. Klungre and D. Bailey (2010), who used 'offset-box' integrals (see Appendix A) to achieve numerical values:

$$\Delta(1, C_2(0)) \;=\; 0.63644048(5)\ldots,$$

$$\Delta(1, C_2(1)) \;=\; 0.553861543(7)\ldots,$$

where the symbol (digit) means it is questionable. By contrast, the full-square classical case is known exactly [3]

$$\Delta(1, C_2(2)) \;=\; \Delta_2(1) \;=\; \frac{1}{15}\left(2+\sqrt{2}+5\log\left(1+\sqrt{2}\right)\right) \;=$$

$$0.521405433164721\ldots,$$

where fractal dimension and expected separation are both monotonically ordered over the three SCS cases. (We have previously, though, by way of Remark demolished any general monotonicity-ordering conjecture.)

2. Application of the high-precision Algorithm 1 in Section 8.3 for the $(n = 2)$-dimensional dust $C_2(0)$ involves the specific instance (note $p = 1$ for this SCS), with q sufficiently large: $B(s, C_2(0)) \approx$

$$\frac{1}{3^{(q-1)s}4^{q-1}(4 \cdot 3^s - 1)} \sum_{\substack{U(c_k) \le P_k \\ (c_1,\ldots c_p) \neq (\mathbf{0}_n,\ldots,\mathbf{0}_n)}} |(\mathbf{1/2})_n + c_1 3^{q-1} + c_2 3^{q-2} + \cdots + c_q|^s, \tag{55}$$

This approach leads via the algorithm to *rigorous* bounds such as

$$\frac{791059}{1000000} \; < \; B(1, C_2(0)) \; < \; \frac{791062}{1000000}.$$

The approximation scheme of the algorithm, on the other hand, yields results (using multiplicity $q \ge 10$) such as

$$\begin{aligned}
B(4, C_2(0)) &= 0.82500000000000000(0), \\
B(1, C_2(0)) &= 0.7910607171001881694140(5)\ldots, \\
B(1/2, C_2(0)) &= 0.857591546196368041 62(5)\ldots, \\
B(-1, C_2(0)) &= 3.228510425537564621 73(5)\ldots, \\
B(-12618595/10000000, C_2(0)) &= 105529978\,.\,23182819(5)\ldots, \\
B(-2, C_2(0)) &= -0.7222518765084439(9)\ldots, \\
B(-3, C_2(0) &= -0.1820952173493284(1)\ldots.
\end{aligned}$$

where only the parenthetic digit is in doubt. This is evidently very difficult to match in precision using Monte Carlo (MC) methods. (Of course, MC methods are still useful, see the Appendix, as strong checks on any other algorithm.)

Note that the exact value of $B(4, C_2(0))$ is 33/40, so the reported value lends credibility to the algorithm. Note also: The B values for sufficiently negative s are *negative*—for these are analytic continuation values to the left of the pole at $s = \log_3 4$;note a B value in excess of 10^8 for s near this pole is on the list above.

3. We have been able to apply self-similarity expansions to effect more precise box-integral values. By self-similarity expansions we mean use of formulae such as the following, appropriate for a function $f(x, y)$ with the fractal $C_2(0)$ assumed:

(56)
$$\frac{11}{3}\,\langle f(x,y)\rangle \;=\left\langle f\left(\frac{x+2}{3},\frac{y}{3}\right)\right\rangle \;+\;\left\langle f\left(\frac{x}{3},\frac{y+2}{3}\right)\right\rangle \;+\;\left\langle f\left(\frac{x+2}{3},\frac{y+2}{3}\right)\right\rangle .$$

One uses the binomial expansion on the right-hand-side and inserts known, exact even-power moments. One may even apply self-similarity a few times recursively to obtain very intricate expansions with perhaps with superior convergence. In this way we achieved (leaving out the symbolic/numeric details attendant on 2-dimensional Taylor expansions):

$$\Delta(1, C_2(0)) \;=\; 0.6364404856978953103681371149310 19(3)\ldots .$$

Though this is probably too imprecise to allow a modern experimental closed-form search, it is nevertheless hard to imagine obtaining such 30+ decimal resolution via direct point-counting or offset-box summations.

This notion of moment expansions suggests there may be a sharp improvement to Algorithm 1; namely, instead of forcing $r \to (\mathbf{1/2})_n$, the centroid value, we can attempt expansion around the centroid and use known even moments. Our best precision to date for $(n = 2)$ dimensions being the 32 digits for $\Delta(1, C_2(0))$ above indicates that such future research is called for.

4. This self-similar expansion method is especially instructive in $(n = 1)$-dimensional cases. We know from Section 8 that for $d := r - 1/2$,

$$B(1/2, C_1(0)) \;=\; \frac{2}{2 - \frac{1}{\sqrt{3}}} \sqrt{\frac{5}{6}} \left\langle \sqrt{1 + \frac{2d}{5}} \right\rangle .$$

Binomial expansion of the d-dependent term here, together with insertion into the expansion of the d-moments, results in extreme precision in reasonable time, e.g., $B(1/2, C_1(0)) =$

$$0.64005103867441304629177740765053368874421733198584478254239 8 \ldots$$

with many more decimals possible. Alternatively, the series (47) leads to the same numerical results.

By contrast, estimation with fractional s in higher dimensions is trickier. Eeen for $n = 2$, $s = -1$ we have not been able to do any better than

$$\Delta(-1, C_2(0)) \;=\; 3.927(1) \ldots$$

Incidentally, this expectation of (separation)$^{-1}$—speaking formally—should agree with

$$\Delta(-1, C_2(0)) \;= \frac{2}{\pi} \int_0^\infty \int_0^\infty \frac{G(u)^2 G(v)^2}{\sqrt{u^2 + v^2}} \mathrm{d}u \mathrm{d}v,$$

where we refer to the kernel $G(w) :=\; {}_1G_0(w) = \prod_{m \geq 1} \cos(w/3^m)$. yet we have been unable to get even the rough value 3.927... via quadrature.

5. Indeed such numerical quadrature is for whatever reason generally problematic. Take for example, the known fact (as have derived) that $\Delta(1, C_1(0)) = 2/5$, leading to the peculiar integral identity

$$\int_0^\infty \frac{\cos k + k \sin k - 1}{k^2} G(k)^2 \, \mathrm{d}k \;=\; \frac{\pi}{5},$$

which, again, does not seem to yield readily to numerical quadrature techniques beyond just a few good decimals. ◇

10 Some open questions

We finish by emphasizing some outstanding questions:

- How can we get expectations such as $\Delta(1, C_2(0))$ to enough accuracy (say 100+ decimals) for experimental-mathematical analysis as explored in [6]? (Note the final observation of Example 12,)3) on possible refinements on Algorithm 1.)

- It is shown in [11] that if the standard Cantor set is charged (say with a total charge of +1), then the electrostatic potential at the position $(0, y)$—so directly above the left-hand edge of $C_1(0)$—is given by

$$V(0, y) \;=\; \frac{1}{2\pi} \int_0^\infty J_0(yk)\, G_1(k)\, \mathrm{d}k,$$

  with ${}_1G_1$ as in Section 6 and J_0 the Bessel function. To date, this integral has not been evaluated, even asymptotically. However, it is known that $V(0, y)$ behaves something like $1/y^{1-\delta}$ where $\delta = \log_3 2$. Might any of the new techniques in the present paper apply?

- For brain-synapse analysis, we would like to know at least a good numerical values for $\Delta(s, C_3(P))$—meaning separation moments in $(n = 3)$ embedding dimensions—and $s = -2, -1, 1$. It would be useful, therefore. to work out a Δ-analogue of ALgorithm 1.

- How much can we build on these results to evaluate expectations on a larger class of fractal sets embedded in the unit hypercube? Perhaps on all fractals covered by Theorem 1.

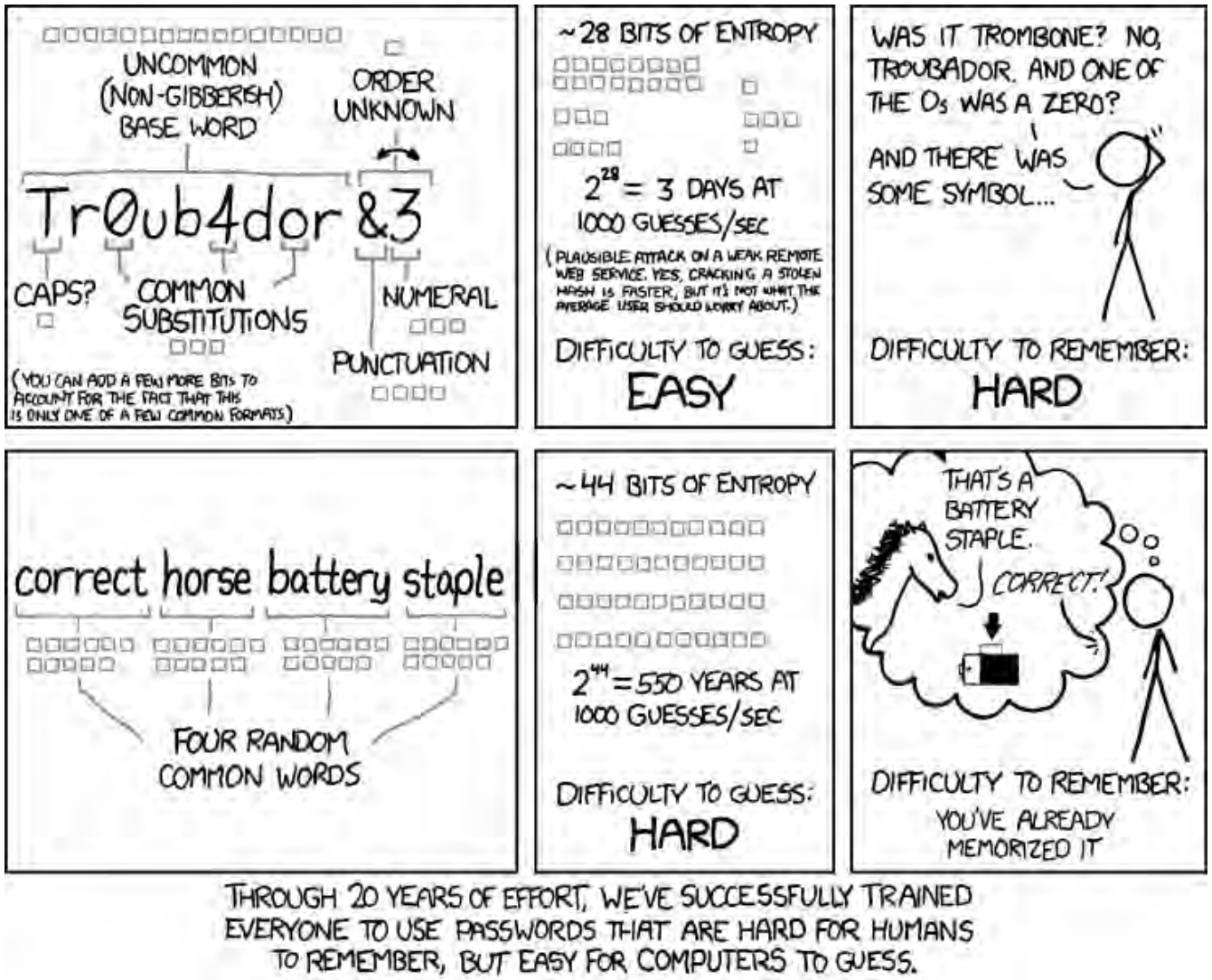

Acknowledgements The authors are grateful to Roland Girgensohn for bringing Theorem 1 to our attention and thus suggesting a more elegant approach to the proof of Proposition 1. They are also indebted to Dirk Nuyens and Josef Dick for discussions on Monte Carlo integration. Thomas Wieting aided us generously in matters of fractal theory.

References

[1] R.S. Anderssen et al, *Concerning* $\int_0^1 \cdots \int_0^1 (x_1^2 + \cdots + x_k^2)^{1/2} \mathrm{d}x_1 \cdots \mathrm{d}x_k$ *and a Taylor Series Method*, SIAM Journal on Applied Mathematics **30** (1976), no. 1, 22-30.

[2] D.H. Bailey, J.M. Borwein and R.E. Crandall, *Advances in the theory of box integrals*, Mathematics of Computation **79** (2009), 1839-1866.

[3] D.H. Bailey, J.M. Borwein and R.E. Crandall, *Box integrals*, Journal of Computational and Applied Mathematics **206** (2007), 196-208.

[4] M. Barnsley, *Fractals everywhere.* Academic Press, Inc., Boston, MA, 1988.

[5] A.K. Basu, *Measure Theory and Probability*, PHI Learning Pvt. Ltd., 2004 p.113.

[6] J.M. Borwein and D.H. Bailey, *Mathematics by Experiment: Plausible Reasoning in the 21st Century*, A.K. Peters Ltd. Second expanded edition, September 2008.

[7] J.M. Borwein, D.H. Bailey and R. Girgensohn, *Experimentation in Mathematics: Computational Paths to Discovery*, A.K. Peters Ltd, 2004.

[8] J.M. Borwein and R. Girgensohn, *Functional equations and distribution functions (for Janos Aczel's 70th Birthday*, Results in Mathematics **26** (1994), 229-237.

[9] J.M. Borwein, O. Chan and R.E. Crandall, *Higher-dimensional box integrals*, Experimental Mathematics **19** (2010), no. 4, 431-446.

[10] R.E. Crandall, *On the fractal distribution of brain synapses*, http://www.perfscipress.com/papers/Synapses.pdf and to appear, Computational and Analytical Mathematics, Proceedings, in Springer Series in Mathematics and Statistics, 2013.

[11] R.E. Crandall, *Theory of box series*, in *Scientific reflections: Selected multidisciplinary works*, PSIpress, 2011.

[12] R.E. Crandall, *Topics in Advanced Scientific Computation*, Springer, New York, (1997).

[13] K. Falconer, *Fractal Geometry: Mathematical Foundations and Applications (2nd edition)*, John Wiley & Sons, West Sussex (2003).

[14] *How Mathematics Can Reveal Brain Structure and Diagnose Brain Health*. 5th June 2012. Available at http://www.sciguru.com/newsitem/13858/how-mathematics-can-reveal-brain-structure-and-diagnose-brain-health, accessed 11th July 2012.

A Box integral data for SCS cases

A.1 Scatterplots of second-order box integrals vs fractal dimension

The separation moments $B(2, C_n(P))$ and $\Delta(2, C_n(P))$ (computed using Theorem 4) and fractal dimension (computed using Proposition 7) of various SCSs were plotted for embedding dimensions $n = 2$ and 3. The resulting scatterplots are shown below.

A.2 Exact rational values and numerical verification for second-order expectations

Below, for a selection of string-generated Cantor sets $C_n(P)$, we present data comprising fractal dimensions $\delta(C_n(P))$ and second-order moments $B(2, C_n(P))$ and $\Delta(2, C_n(P))$ for embedding dimension $n = 1$, 2 and 3, with entries arranged in order of increasing fractal dimension. All such quantities are rational and were computed exactly—fractal dimensions via Proposition 7, and separation moments via Theorem 4. Decimal equivalents (to six-digit accuracy) are included, together with results of Monte-Carlo computations, as a check.

1. One possible Monte-Carlo approach is to utilize a uniform $(0, 1)$ pseudorandom number generator to generate pairs of n-tuples at random, then check each pair of n-tuples so generated to see if it is "admissible" for the given set $C_n(P)$. This is certainly a relatively simple and straightforward scheme to code on a computer, and can be used effectively in cases where the average "density" of the fractal set is not too small.

   – The disadvantage of this scheme is that for many fractal Cantor sets that one might wish to examine, the density is so small that only a microscopic fraction of the n-tuple pairs so generated in each trial are admissible. In such cases, thousands or even millions of pairs of n-tuples must be generated to find just one admissible pair, and yet millions of such valid pairs must be generated to obtain reliable mean statistics.

2. A second approach, which we adopted below, is, for each case to be studied, to first construct a table of all admissible columns c_k for each of the components of P, and then, for each of a large number of trials, and for each ternary column $1 \leq k \leq 20$ of a single trial,

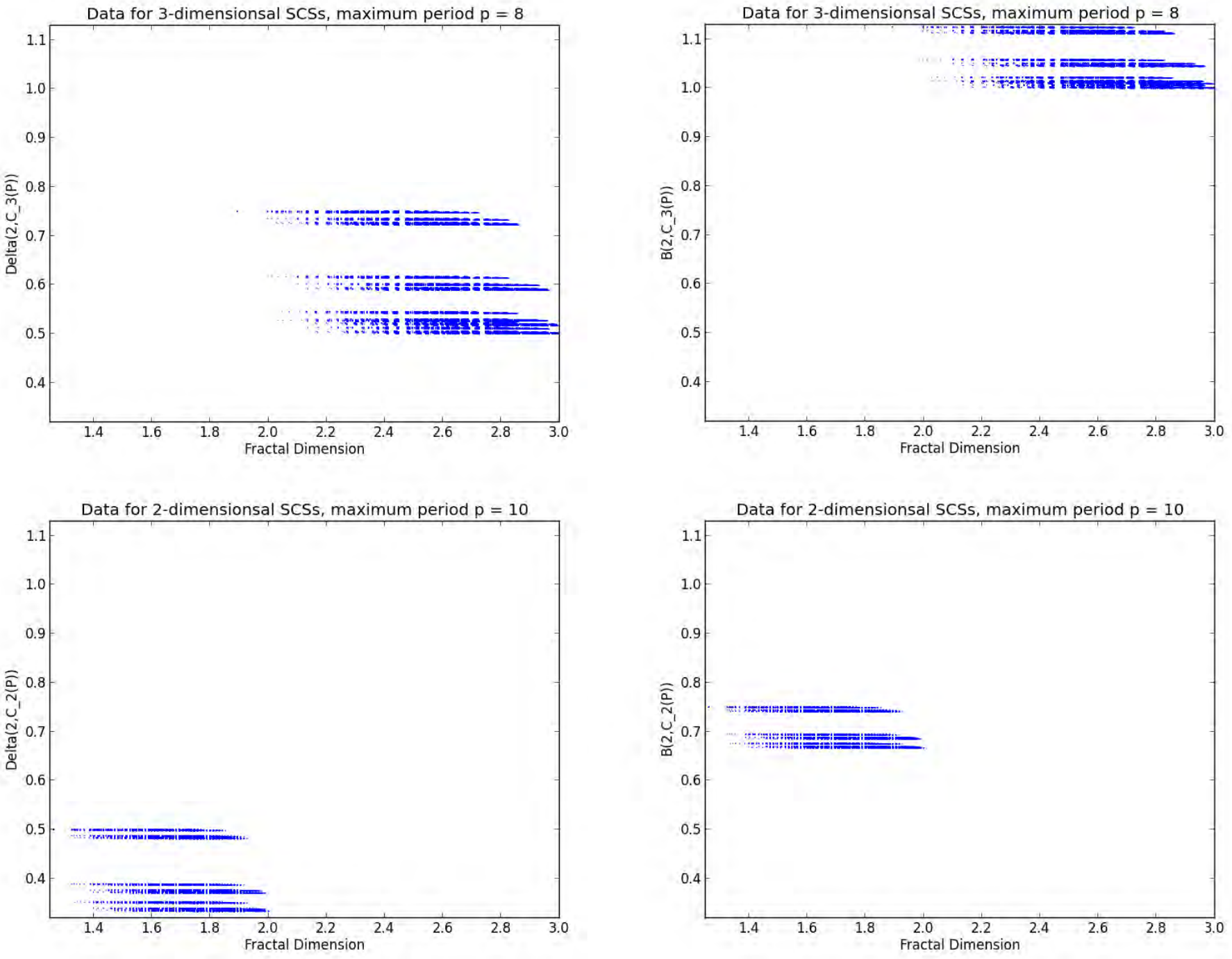

Figure 6: Separation moments plotted against fractal dimensions for SCSs. Top: separation moments $\Lambda(2, C_3(P))$ (left) and $B(2, C_3(P))$

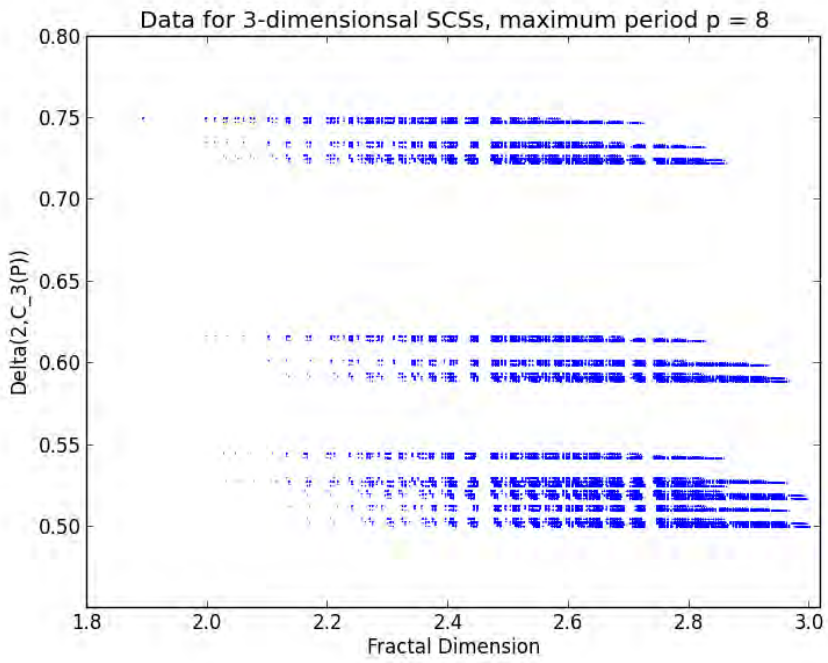

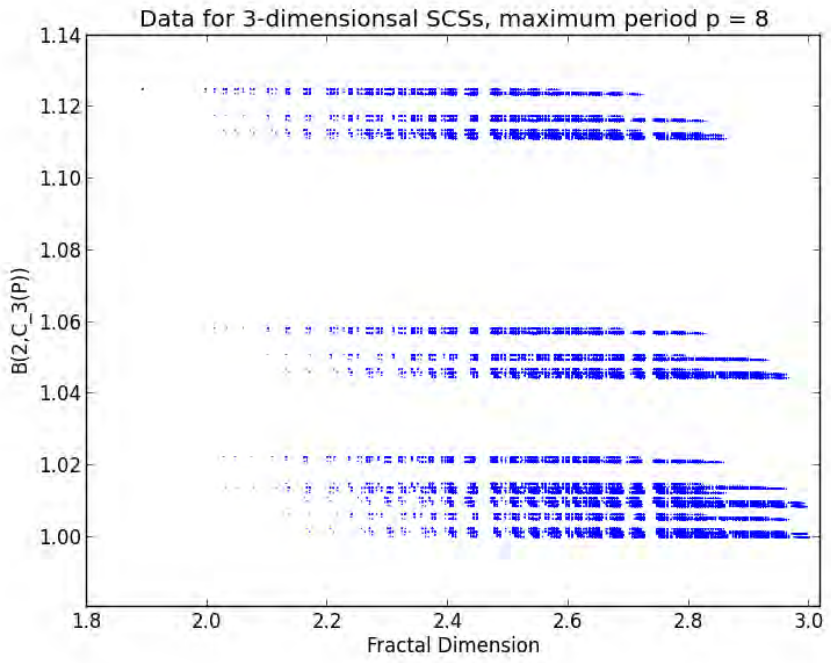

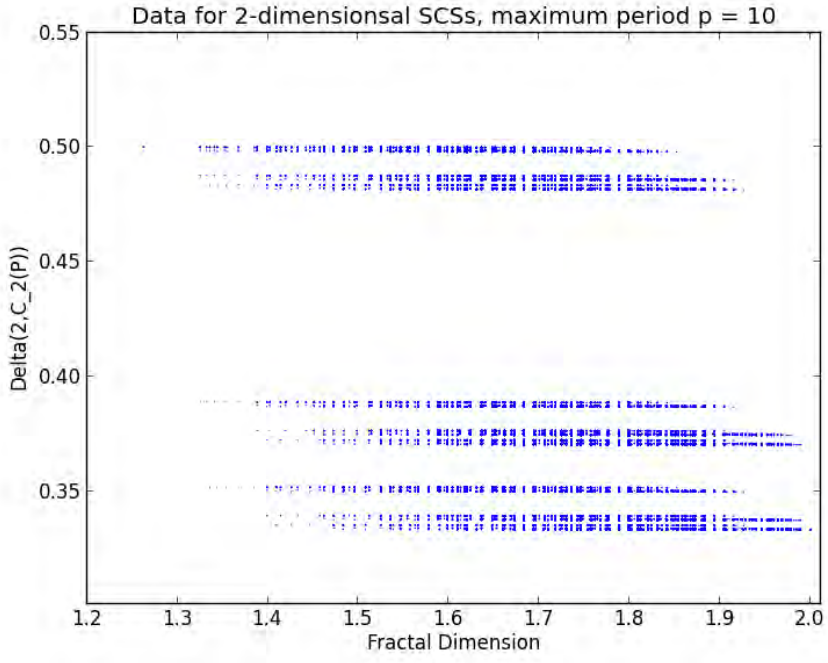

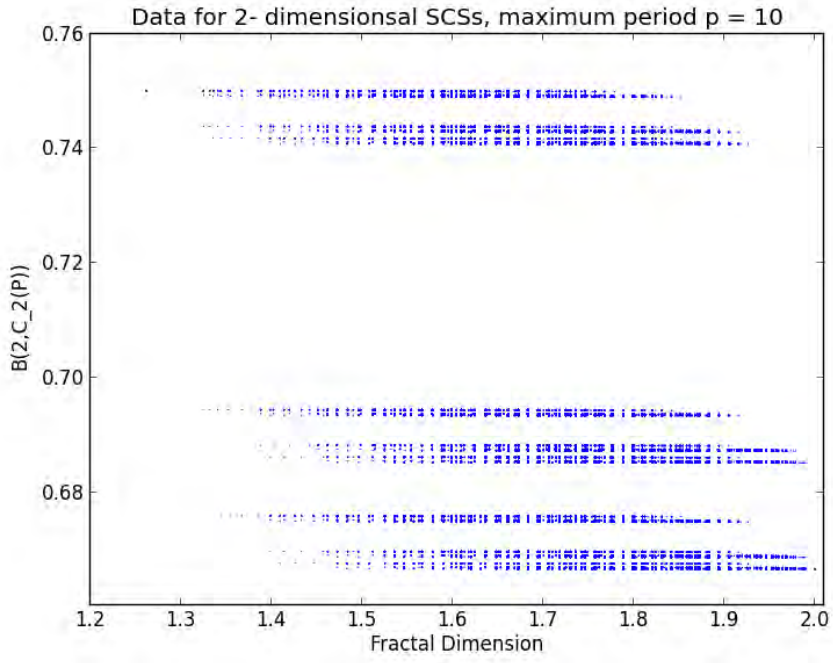

Figure 7: Separation moments plotted against fractal dimensions for SCSs. Top: separation moments $\Delta(2, C_3(P))$ (left) and $B(2, C_3(P))$

pseudorandomly select an admissible column from the appropriate table. While coding this scheme is much more complicated that the more straightforward scheme, it has the distinct advantage that each pair of n-tuples is guaranteed to be admissible.

- We have tabulated our results, with the columns headed by "Numeric" giving Monte-Carlo results for $B(2, C_n(P))$ and $\Delta(2, C_n(P))$. In each line, figures are based on a computation of 10^9 pseudorandom pairs of admissible n-tuples, each to 20 ternary digit precision. Note that 20 ternary digit precision corresponds to roughly 9.5 decimal digit precision, which is adequate given that fact that even with 10^9 pseudorandom trials per case, only about 5 accurate digits can be expected in the output means. At the bottom of each of the three tables are statistics giving the *maximum* and *root-mean-square* error for the Monte-Carlo results in the table. We observe that theory and computation mesh very well.
- As a final set of results, we also exhibit, in Table 6, a few validating results for the box integrals $B_n(s, C_n(P))$, kindly provided to the authors by Dirk Nuyens, who employed a multi-level Monte-Carlo scheme to compute moments for $s = 1$, $s = 2$ and $s = 1/2$, for various $C_n(P)$.

3. We mention one other approach, which was taken by V. Klungre in Example 12 of the previous section. Klungre utilized a *Mathematica* program to compute the mean distance, in any given dimension n, between points in two square (or cube, etc.) Cantor patches. He then recursively extended this scheme up to dimension 9. While the results so produced are very accurate, so much computation is required for a single case that it is not practical for a large number of cases, as we required below.

We are investigating more sophisticated quasi-Monte-Carlo schemes, but do not yet have any results.

A.2.1 Tabulated data for $n = 1$ (generating string period ≤ 4), with numeric Monte-Carlo results based on 10^9 trials

P	$\delta(C_1(P))$	$B(2, C_1(P))$			$\Delta(2, C_1(P))$		
	Decimal	Rational	Decimal	Numeric	Rational	Decimal	Numeric
0	0.630930	$\frac{3}{8}$	0.375000	0.375013	$\frac{1}{4}$	0.250000	0.250009
0001	0.723197	$\frac{7379}{19680}$	0.374949	0.374941	$\frac{2459}{9840}$	0.249898	0.249904
0010	0.723197	$\frac{2457}{6560}$	0.374543	0.374543	$\frac{817}{3280}$	0.249085	0.249080
0100	0.723197	$\frac{2433}{6560}$	0.370884	0.370887	$\frac{793}{3280}$	0.241768	0.241765
1000	0.723197	$\frac{2217}{6560}$	0.337957	0.337937	$\frac{577}{3280}$	0.175915	0.175928
001	0.753953	$\frac{409}{1092}$	0.374542	0.374552	$\frac{68}{273}$	0.249084	0.249092
010	0.753953	$\frac{135}{364}$	0.370879	0.370877	$\frac{22}{91}$	0.241758	0.241751
100	0.753953	$\frac{123}{364}$	0.337912	0.337895	$\frac{16}{91}$	0.175824	0.175824
0011	0.815465	$\frac{737}{1968}$	0.374492	0.374486	$\frac{245}{984}$	0.248984	0.248989
01	0.815465	$\frac{89}{240}$	0.370833	0.370836	$\frac{29}{120}$	0.241667	0.241661
0110	0.815465	$\frac{243}{656}$	0.370427	0.370429	$\frac{79}{328}$	0.240854	0.240850
10	0.815465	$\frac{27}{80}$	0.337500	0.337481	$\frac{7}{40}$	0.175000	0.175014

1001	0.815465	$\frac{665}{1968}$	0.337907	0.337894	$\frac{173}{984}$	0.175813	0.175812
1100	0.815465	$\frac{219}{656}$	0.333841	0.333825	$\frac{55}{328}$	0.167683	0.167686
011	0.876977	$\frac{809}{2184}$	0.370421	0.370397	$\frac{263}{1092}$	0.240842	0.240847
101	0.876977	$\frac{737}{2184}$	0.337454	0.337442	$\frac{191}{1092}$	0.174908	0.174904
110	0.876977	$\frac{243}{728}$	0.333791	0.333781	$\frac{1}{6}$	0.167582	0.167583
0111	0.907732	$\frac{7289}{19680}$	0.370376	0.370350	$\frac{2369}{9840}$	0.240752	0.240757
1011	0.907732	$\frac{6641}{19680}$	0.337449	0.337440	$\frac{1721}{9840}$	0.174898	0.174903
1101	0.907732	$\frac{6569}{19680}$	0.333791	0.333765	$\frac{1649}{9840}$	0.167581	0.167574
1110	0.907732	$\frac{2187}{6560}$	0.333384	0.333386	$\frac{547}{3280}$	0.166768	0.166774
1	1.000000	$\frac{1}{3}$	0.333333	0.333333	$\frac{1}{6}$	0.166667	0.166671
Max error				0.000033			0.000026
RMS error				0.000014			0.000008

A.2.2 Tabulated data for $n = 2$ (generating string period ≤ 2), with numeric Monte-Carlo results based on 10^9 trials

P	$\delta(C_2(P))$	$B(2, C_2(P))$			$\Delta(2, C_2(P))$		
	Decimal	Rational	Decimal	Numeric	Rational	Decimal	Numeric
0	1.26186	$\frac{3}{4}$	0.750000	0.750012	$\frac{1}{2}$	0.500000	0.500036
01	1.577324	$\frac{119}{160}$	0.743750	0.743744	$\frac{39}{80}$	0.487500	0.487478
10	1.577324	$\frac{111}{160}$	0.693750	0.693716	$\frac{31}{80}$	0.387500	0.387514
02	1.630930	$\frac{89}{120}$	0.741667	0.741664	$\frac{29}{60}$	0.483333	0.483325
20	1.630930	$\frac{27}{40}$	0.675000	0.674983	$\frac{7}{20}$	0.350000	0.349996
1	1.892789	$\frac{11}{16}$	0.687500	0.687486	$\frac{3}{8}$	0.375000	0.374998
12	1.946395	$\frac{329}{480}$	0.685417	0.685414	$\frac{89}{240}$	0.370833	0.370830
21	1.946395	$\frac{107}{160}$	0.668750	0.668743	$\frac{27}{80}$	0.337500	0.337494
2	2.000000	$\frac{2}{3}$	0.666667	0.666646	$\frac{1}{3}$	0.333333	0.333335
Max error				0.000057			0.000036
RMS error				0.000024			0.000010

A.2.3 Tabulated data for $n = 3$ (generating string period ≤ 2), with numeric Monte-Carlo results based on 10^9 trials

P	$\delta(C_3(P))$	$B(2, C_3(P))$			$\Delta(2, C_3(P))$		
	Decimal	Rational	Decimal	Numeric	Rational	Decimal	Numeric
0	1.892789	$\frac{9}{8}$	1.125000	1.124983	$\frac{3}{4}$	0.750000	0.749994
01	2.309811	$\frac{447}{400}$	1.117500	1.117460	$\frac{147}{200}$	0.735000	0.734995
10	2.309811	$\frac{423}{400}$	1.057500	1.057481	$\frac{123}{200}$	0.615000	0.614989
02	2.429218	$\frac{579}{520}$	1.113462	1.113436	$\frac{189}{260}$	0.726923	0.726925
20	2.429218	$\frac{531}{520}$	1.021154	1.021104	$\frac{141}{260}$	0.542308	0.542313
03	2.446395	$\frac{89}{80}$	1.112500	1.112453	$\frac{29}{40}$	0.725000	0.725009
30	2.446395	$\frac{81}{80}$	1.012500	1.012502	$\frac{21}{40}$	0.525000	0.525011
1	2.726833	$\frac{21}{20}$	1.050000	1.049967	$\frac{3}{5}$	0.600000	0.599985
12	2.846240	$\frac{5439}{5200}$	1.045962	1.045915	$\frac{1539}{2600}$	0.591923	0.591917
21	2.846240	$\frac{5271}{5200}$	1.013654	1.013606	$\frac{1371}{2600}$	0.527308	0.527303
13	2.863417	$\frac{209}{200}$	1.045000	1.045028	$\frac{59}{100}$	0.590000	0.589982
31	2.863417	$\frac{201}{200}$	1.005000	1.004979	$\frac{51}{100}$	0.510000	0.509998

2	2.965647	$\frac{105}{104}$	1.009615	1.009601	$\frac{27}{52}$	0.519231	0.519224
23	2.982824	$\frac{1049}{1040}$	1.008654	1.008633	$\frac{269}{520}$	0.517308	0.517303
32	2.982824	$\frac{1041}{1040}$	1.000962	1.000925	$\frac{261}{520}$	0.501923	0.501918
3	3.000000	1	1.000000	0.999960	$\frac{1}{2}$	0.500000	0.499983
Max error				0.000065			0.000032
RMS error				0.000031			0.000012

C	$B(2,C)$	$B(1,C)$	$B(1/2,C)$
$C_3(0)$	1.12500	1.00501	0.98359
$C_3(1)$	1.05000	0.97909	0.97522
$C_3(2)$	1.00961	0.96424	0.96957
$C_3(3)$	1.00000	0.96059	0.96811
$C_2(0)$	0.75000	0.79106	0.85759
$C_2(1)$	0.68750	0.77261	0.85778
$C_2(2)$	0.66667	0.76520	0.85581
$C_1(0)$	0.37500	0.50000	0.64005
$C_1(1)$	0.33333	0.50000	0.66667
$C_3(01)$	1.11750	1.00196	0.98229
$C_3(10)$	1.05750	0.98205	0.97648
$C_3(02)$	1.11346	1.00028	0.98151
$C_2(01)$	0.74375	0.78846	0.85735
$C_2(10)$	0.69375	0.77507	0.85830
$C_2(02)$	0.74167	0.78749	0.85700
$C_2(20)$	0.67500	0.76846	0.85662
$C_2(12)$	0.68542	0.77174	0.85748
$C_2(21)$	0.66875	0.76605	0.85610

C	$\Delta(2,C)$	$\Delta(1,C)$	$\Delta(1/2,C)$
$C_3(01)$	0.3675	0.5969	0.7694
$C_3(10)$	0.3075	0.5404	0.7299
$C_3(02)$	0.3634	0.5946	0.7683

Table 6: The expectation integrals for various s, computed by Dirk Nuyens (for B) and Josef Dick (for Δ,).